Bone 154 (2022) 116256

Contents lists available at ScienceDirect

Bone

journal homepage: www.elsevier.com/locate/bone

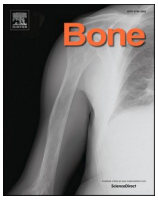

Recent approaches towards bone tissue engineering

F. Raquel Maia [*], Ana R. Bastos, Joaquim M. Oliveira, Vitor M. Correlo, Rui L. Reis

[a] 3B's Research Group, I3Bs-Research Institute on Biomaterials, Biodegradables and Biomimetics of University of Minho, Headquarters of the European Institute of Excellence on Tissue Engineering and Regenerative Medicine, AvePark, Parque de Ciência e Tecnologia, Zona Industrial da Gandra, 4805-017 Barco, Guimarães, Portugal

[b] ICVS/3B's PT Government Associate Laboratory, Braga, Guimarães, Portugal

ARTICLE INFO

Keywords:
Bone tissue engineering
Scaffolds
3D printing
3D bioprinting
Spheroids
Vascularized strategies

ABSTRACT

Bone tissue engineering approaches have evolved towards addressing the challenges of tissue mimetic requirements over the years. Different strategies have been combining scaffolds, cells, and biologically active cues using a wide range of fabrication techniques, envisioning the mimicry of bone tissue. On the one hand, biomimetic scaffold-based strategies have been pursuing different biomaterials to produce scaffolds, combining with diverse and innovative fabrication strategies to mimic bone tissue better, surpassing bone grafts. On the other hand, biomimetic scaffold-free approaches mainly foresee replicating endochondral ossification, replacing hyaline cartilage with new bone. Finally, since bone tissue is highly vascularized, new strategies focused on developing pre-vascularized scaffolds or pre-vascularized cellular aggregates have been a motif of study. The recent biomimetic scaffold-based and scaffold-free approaches in bone tissue engineering, focusing on materials and fabrication methods used, are overviewed herein. The biomimetic vascularized approaches are also discussed, namely the development of pre-vascularized scaffolds and pre-vascularized cellular aggregates.

1. Introduction

Bone tissue can self-heal upon the damage, such as fractures or minor defects, without giving rise to scar tissue. But, this phenomenon is only observed when the length of the damage does not go beyond double the diameter of the affected bone [1,2]. More significant defects can result in scar tissue formation or even in longstanding weaknesses, requiring clinical intervention, which results in a substantial burden for the patients. Several approaches using bone autografts, allografts, or synthetic bone substitutes are currently used to treat such significant defects [2]. Even so, these strategies present some limitations. For example, the use of autografts can result in donor site morbidity, infections at the intervention site, or pain for the patient, while the use of allografts presents the risk of disease transmission [2]. In the case of bone substitutes such as prostheses, they usually require subsequent revision [3]. To tackle these limitations, different tissue engineering approaches have been studied to develop improved strategies focused on the use of scaffolds, cells, and biologically active cues for bone tissue regeneration [4]. Those strategies are expected to induce the repair and regeneration of bone tissue. The mimicry of bone tissue has been one of the main focuses of bone tissue engineering, envisioning the achievement of a more physiologically relevant strategy and consequently a higher hypothesis of success [5]. Bone extracellular matrix (ECM) is a natural composite containing a polymeric matrix, composed mainly of collagen type I and a mineral component composed mainly of hydroxyapatite (HAp) (Fig. 1) [6]. Surrounded by this hybrid environment, different types of cells can be found, namely osteoblasts, osteoclasts, and osteocytes. It is this complex structure that bone tissue engineering approaches are trying to copycat to enable and support new and functional bone tissue growth.

Different sources have been pursued to develop improved biodegradable polymeric biomaterials to produce scaffolds and matrices for bone tissue engineering. Such systems would act as temporary artificial ECM, degrading and adsorbing by the body as the new bone is formed [7].

Biomaterials can be obtained from natural sources, as in the case of alginate, collagen, or nano-hydroxyapatite (nHA), or can be produced synthetically as poly (ethylene glycol) (PEG) or poly(ε-caprolactone) (PCL) [8–13]. Also, they can be used individually or in combination to produce the scaffold that best mimics bone tissue's ECM, enabling cell attachment, proliferation, and differentiation, while conferring

* Corresponding author at: 3B's Research Group, I3Bs-Research Institute on Biomaterials, Biodegradables and Biomimetics of University of Minho, Headquarters of the European Institute of Excellence on Tissue Engineering and Regenerative Medicine, AvePark, Parque de Ciência e Tecnologia, Zona Industrial da Gandra, 4805-017 Barco, Guimarães, Portugal.
E-mail address: raquel.maia@i3bs.uminho.pt (F.R. Maia).

https://doi.org/10.1016/j.bone.2021.116256
Received 1 June 2021; Received in revised form 19 October 2021; Accepted 9 November 2021
Available online 12 November 2021

appropriate mechanical support [9,10,12]. Regarding scaffold-based approaches, two main strategies can be found upon revision of current literature, studies that focus on the seeding of cells within the developed scaffolds or studies that focus on the recruitment of surrounding cells upon implantation of scaffolds alone [14,15]. In this sense, the last-mentioned systems can be osteoinductive, enabling the recruitment of osteoprogenitor cells and their differentiation along osteoblastic lineage, and osteoconductive enabling the osteoprogenitor cells surrounding the scaffold to colonize it and gradually replace it with newly formed bone tissue [16]. Additionally, both options can include biologically active cues [17–19]. Concerning the type of cells used, stem cells are the most often selected due to their inherent ability to differentiate along the osteoblastic lineage [20,21]. Furthermore, stem cells could be obtained from adult and fetal tissues. Nevertheless, adult stem cells, such as bone marrow mesenchymal stem cells (BMSCs) and adipose-derived mesenchymal stem cells (ASCs), present fewer ethical concerns and have been studied extensively for bone regeneration strategies [21]. BMSCs are usually obtained from the iliac crest, using invasive procedures resulting in low isolation yields. In contrast, ASCs are obtained from adipose tissue through minimally invasive procedures, usually from liposuctions, resulting in high isolation yields [22]. Noteworthy, the number of total cells obtained from liposuctions will depend on the size of sample available, which in many cases results in a lower amount of ASCs compared with BMSCs. In both cases, the osteogenic differentiation capabilities decrease with the increase of culture passage, being maximum between passage 3–4 for ASCs and passage 6 for BMSCs [21]. Nevertheless, in the particular case of bone tissue engineering, it is known that BMSCs presents higher osteogenic markers and mineralization deposits than ASCs [21,23]. In the case of bioactive cues, such as bone morphogenetic proteins (BMPs), they can direct cells' behavior by stimulating the proliferation of cells and the differentiation or even cell migration [24,25]. In this sense, stimulating signaling cascades by adding such cues may provide on-demand features to the produced scaffolds, improving bone tissue regeneration [17]. Nevertheless, it is essential to highlight that, despite their favorable influence, cells and biological cues can result in higher costs and ethical constraints, making strategies based on just biomaterials- faster translated into the clinics. However, since bone tissue is highly vascularized, new strategies are being pursued to include vascular features in the developed scaffolds, aiming to improve the success rates of bone regeneration approaches [26]. In fact, creating a vascular system would enable the supply of nutrients and removal of biological waste, mimicking the osteogenic cells' microenvironment.

In alternative to scaffold-based approaches, a different Tissue Engineering research line focused on investigating bone tissue developmental programs has been investigated [27,28]. This line of research is usually denominated as scaffold-free approaches, and their main characteristics will be highlighted in this review. In these strategies, the regeneration of bone would be obtained through the recapitulation of the native endochondral bone tissue developmental program. For that, cells would create their relevant bone tissue ECM upon stimulation with proper molecular and mechanical cues, usually resulting in tissue with several similarities in terms of morphology, structure, and function to the native one.

The current reports dealing with the biomimetic scaffold-based and scaffold-free approaches for bone tissue engineering are overviewed herein. In addition, it is described the biodegradable polymeric materials and fabrication methods used and the biomimetic vascularized approaches that have been exploited, namely the development and use of pre-vascularized scaffolds and pre-vascularized cellular aggregates.

2. Biomimetic scaffold-based strategies

As aforementioned considering biomimetic scaffold-based strategies for bone tissue engineering, different biomaterials have been used for the production of the scaffolds that better mimic bone tissue, surpassing bone grafts shortcomings, namely limited availability or donor site morbidity [29]. Nevertheless, in short, an ideal scaffold should comprise some intrinsic features, including being biocompatible, biodegradable, and having mechanical properties similar to bone tissue [30].

In addition, the successful development of a functionally engineered tissue requires the complete colonization of the scaffold by the seeded cells. Thus, the scaffold must support cells adhesion and proliferation, differentiation, and ECM deposition, resulting in its gradual replacement by the native tissue [30]. For that to occur, pore size and porosity must be adequate to support cell migration and the ingrowth of surrounding tissues and enable the supply of nutrients and the release of debris resulting from the metabolic activity of cells [31]. It was demonstrated by Xue et al. [32] that pore sizes bigger than 200 μm resulted in cells aligned with the surface of the pore, while pores with sizes smaller than 100 μm no cellular growth was observed. For so, pores within such range would present improved growth of bone tissue. Nevertheless, other studies demonstrated that bigger pores (>300 μm) resulted in enhanced bone formation [33–35]. Overall, there is no consensus regarding an optimal size that promotes effective bone regeneration. Considering the porosity of the scaffolds, to mimic cancellous bone, the scaffold should present a porosity ranging from 50% to 90% [29,36]. Still, the scaffold should show a porosity around 10% to 30% to mimic the cortical bone.

Moreover, scaffolds should resemble the defect morphology and address all features of the patient's tissue. In more detail, scaffolds must mimic the morphological and compositional elements of the patient's healthy bone tissue to guarantee a more successful approach [37]. For example, it has been shown by Stuckensen et al. [37] that scaffolds capable of mimicking the architecture and biochemical composition of the osteochondral and meniscus tissue can direct cells' behavior, inducing their ingrowth and matrix synthesis without the addition of any supplements. Considering a surgical scenario, the optimum scaffold should be easy to handle and adapt to the defect site enabling a precise implant.

2.1. Biomaterials for scaffold production

Different biomaterials ranging from natural and synthetic polymers to bioceramics and their composites have been produced using diverse techniques to mimic as much as possible the features of bone tissue (Fig. 2).

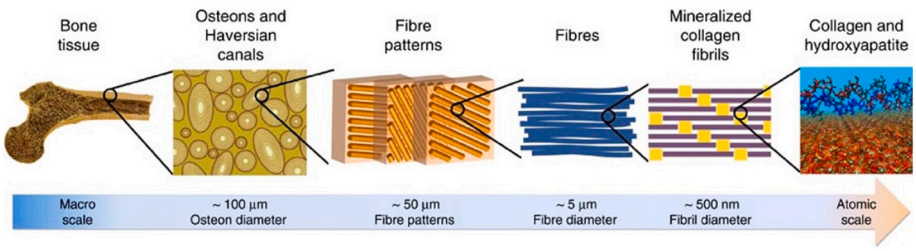

Fig. 1. Schematic representation of bone tissue composition. Hierarchical composition of bone tissue, from macro scale to the atomic scale, showing the collagen fibrils and the HAp. Reprinted with permission from [6] under Creative Commons Attribution License.

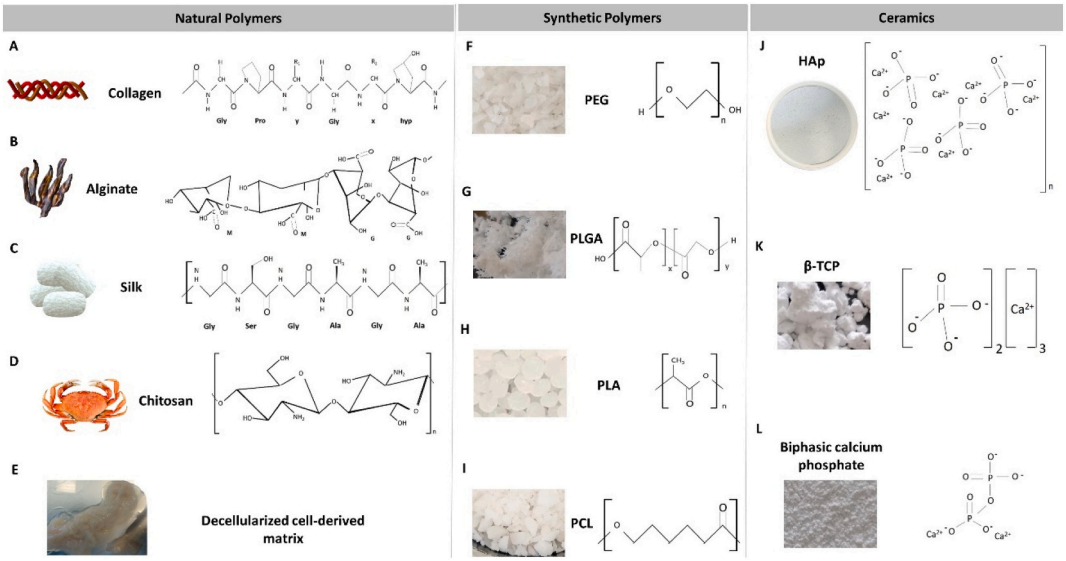

Fig. 2. Representative images of natural polymers, synthetic polymers, and ceramics used for scaffold production. A) Schematic representation of collagen triple helix and its chemical structure; B) Representative image of brown algae that origin alginate and its chemical structure; C) Representative image of *Bombyx mori* silk cocoons that origin silk and its chemical structure; D) Representative image of a crustacean that origins chitosan and its chemical structure; E) Representative image of a decellularized cell-derived matrix; F) Representative image of PEG and its chemical structure; G) Representative image of Poly (lactic acid-*co*-glycolic acid) (PLGA) and its chemical structure; H) Representative image of PLA and its chemical structure; I) Representative image of Poly(ε-caprolactone) (PLC) and its chemical structure; J) Representative image of HAp and its chemical structure; K) Representative image of β-tricalcium phosphate (β-TCP) and its chemical structure; and L) Representative image of biphasic calcium phosphate and its chemical structure.

2.1.1. Natural based polymers

Natural-based polymers can provide native cellular adhesion sites and can mimic the chemical composition of bone tissue to some extent (*e.g.*, collagen), contrary to synthetic polymers that can only offer this scenario upon modification of their backbone with relevant proteins or peptides [38]. Nevertheless, despite these significant advantages, natural-based polymers, such as collagen, alginate, silk, chitosan, and decellularized matrices, often presents batch-to-batch variation and low mechanical properties (Figs. 2 A–E).

Even so, there are currently in the market and used in the clinics, different approaches derived from natural-based polymers, namely MaioRegen® (JRI Orthopaedics Ltd) [39]. This product presents different layers to mimic the osteochondral environment. In more detail, it comprises three layers: the first mimics the cartilage, containing collagen type I, the second layer mimics the calcified cartilage, comprising magnesium-enriched HAp and collagen, and finally, the third layer mimics the subchondral bone, comprising magnesium-enriched HAp. As collagen is the most dominant protein of bone tissue, its use in scaffolds' fabrication has been widely pursued in bone tissue engineering approaches (Fig. 2 A) [40]. Collagen forms a hydrogel in response to the temperature, providing cells with a unique high-water- content environment. Moreover, it presents adhesive and degradable sites, enabling cellular adhesion and, later, the matrix environment remodeling. Nevertheless, collagen-based hydrogels frequently give rise to matrices with low stiffness [40]. To improve the mechanical properties of the hydrogels, additional crosslinking methods, based on chemical mediators or physical events, have been pursued to produce intra or intermolecular bonds [41]. Other approaches to strengthen these hydrogels comprise the production of composite biomaterials. For example, in work published by Jing and colleagues [42], collagen was mixed with carbon nanotubes and HAp. The results have shown that the composite biomaterial presented improved stiffness and osteogenecity by inducing the formation of new bone in a rat calvarial defect.

Another natural-based polymer widely used in bone tissue engineering approaches is alginate [43,44]. Alginate is obtained from brown algae, and its chemical structure is composed of β-D-mannuronate and α-L-guluronate units (Fig. 2 B) [45]. The reaction of guluronate units with divalent cations promotes an egg-box structure, resulting in the gelation of alginate. This ionotropic gelation can be carried out under physiological conditions, allowing the successful entrapment of cells [18,46]. Alginate's mechanical properties are dependent on the ratio between mannuronate and guluronate units. In this sense, more robust hydrogels can be developed by increasing the number of guluronate units. Since alginate is not cleavable by mammalian enzymes, its degradable features rely on replacing the divalent for monovalent ions rather than depending on enzymatic degradation. To overcome this limitation, proteolytically cleavable peptides can be incorporated, promoting cell-mediated degradation [47]. Considering these features, alginate hydrogels can also contain immobilized osteogenic growth factors, as Xu et al. [48] described. In this study, the authors developed double-layered microspheres to promote the sequential release of cell homing factor, stromal cell-derived factor-1 (SDF-1), and the osteoinductive growth factor, bone morphogenetic protein-2 (BMP-2). The results demonstrated that this system enhanced the recruitment of osteogenic cells and improved the development of osteogenic features, such as the increase of alkaline phosphatase (ALP) activity, the production of mineralized modules, and the enhancement of osteogenic-related genes' expression.

Silk is one of the strongest natural fibers, with 0.6 GPa strength [49]. Silk can be obtained from different sources, including spiders and silkworms, and is composed of two main proteins, fibroin, and sericin (Fig. 2 C). Since sericin has been shown to promote allergic reactions, tissue engineering research has been primarily focused on using silk fibroin [50]. Natural silk is exposed to a degumming protocol for extracting silk fibroin, which comprises its immersion into boiling water and salts or detergents, removing the sericin [51]. The resultant silk fibroin includes a heavy chain of ≈350 kDa and a light chain of ≈25 kDa, connected by a disulfide bond. Moreover, this protein presents excellent resistance to deformation and an excellent break strain (4–26%) [52]. Considering such exceptional mechanical properties, silk may match different tissues' elasticity and mechanical strength, making it a suitable material for load-bearing applications, including bone tissue engineering approaches [53]. For example, silk was clinically approved for load-bearing

applications such as surgical meshes, sutures, and garments for dermatological conditions [54]. Nowadays, such features have prompted scientists to use silk to develop scaffolds for applications that need support and load transfer as orthopaedics.

Furthermore, it has been reported that silk fibroin can promote the growth of HAp, emulating the typical constituents of bone tissue, collagen, and calcium phosphate [49,55]. In a different study, Kundu et al. [56] have shown that blending silk fibroin with gellan gum promoted the mineralization of the prepared matrices, improving their features as supports for bone tissue engineering applications.

Chitosan is another natural-based polymer being widely studied for bone tissue engineering applications [57]. Chitosan is a polysaccharide derived from chitin (present in the exoskeletons of crustaceans) upon deacetylation that presents antibacterial properties (Fig. 2 D). It is composed of β-(1–4)-linked D-glucosamine and *N*-acetyl-D-glycosamine groups, forming a hydrogel under physical crosslinking methods based on pH and temperature [58,59]. But the resulting hydrogels present low mechanical properties. Thus, chitosan is often modified or combined with other biomaterials to improve its mechanical properties [60,61]. One example is the work of Zafeiris and co-workers, where they combined chitosan with HAp and proposed to crosslink chitosan with genipin to improve its mechanical properties [61]. The results have shown that the mechanical properties achieved were very similar to those presented by cancellous bone.

Finally, decellularized matrices have gained the attention of researchers due to their complexity, emulating the native bone tissue environment [62,63]. Decellularized matrices are obtained after the removal of all cellular components from harvested bone tissue [64]. The resultant product is highly recognized by cells. Moreover, the decellularization process should preserve the tissue's complex composition, architecture, and vascular system [65].

Cell-derived matrices have also gained the attention of researchers. But, on the contrary to tissue-derived matrices, cell-derived matrices are less complex environments [66]. They do not possess as many factors and thus do not fully mimic the tissue-like architecture (Fig. 2 E). Nevertheless, due to their high availability compared with tissue-derived matrices, more studies have been focused on this type of matrix to develop new tissue engineering approaches [67,68]. Different enzymatic, chemical, and physical methods are usually applied to extract the extracellular matrix, removing all the cellular components to avoid any immunological response without damaging it [69]. One of the main disadvantages relies on its low mechanical properties, demanding further combinations to enhance them, as shown in the work of Carvalho et al. [70]. In this study, researchers combined matrices derived from human mesenchymal stem cells (MSCs) and human umbilical vein endothelial cells (hUVECs) with Poly(ε-caprolactone) (PCL) to produce a matrix with improved mechanical properties for bone tissue engineering applications. The data obtained showed that the developed matrices were able to enhance the osteogenic differentiation of cultured MSCs.

2.1.2. Synthetic polymers

Contrarily to naturally derived polymers, synthetic polymers, such as PEG, Poly (lactic acid-*co*-glycolic acid) (PLGA), poly-lactic acid (PLA), and PCL (Figs. 2 F–I), present improved mechanical properties. Also, it can be modified on-demand to meet the required properties for each strategy [38]. One of the most frequent modifications used is the addition of Arg-Gly-Asp (RGD) peptide. This peptide has been well-known since 1984 when Pierschbacher and Rouslahti identified it as the minimal essential cell-adhesion sequence found in fibronectin [30].

PEG has been highly investigated since it presents highly tunable features (Fig. 2 F) [71]. Nevertheless, the absence of cellular recognition sites requires its further modification with bioactive cues [72]. In addition, PEG can also be combined with other natural-based polymers to acquire cell recognition sites [73]. It can also be combined with ceramics, improving its bioactivity, as described by Chaha et al. [74]. Nevertheless, it was observed that the modification of the polymer with cell adhesion motifs was crucial in promoting cell adhesion.

PLGA is a copolymer of polylactic acid (PLA) and polyglycolic acid (PGA), being the ratio between both the responsible for PLGA properties (Fig. 2 G) [75]. For example, as the amount of lactic acid increases, the solubility of PLGA increases, while as the number of glycolic acid increases, the degradation of PLGA decreases. These accessible tunable features attracted bone tissue engineering researchers [76]. In work reported by Liang and colleagues, PLGA was used to create a bilayer scaffold for osteochondral regeneration approaches [76]. The bilayer scaffold presented one layer of PLGA (cartilage regeneration) and one layer of PLGA combined with Hap (bone regeneration). Upon grafting it into an artificial osteochondral defect, the developed scaffold showed to stimulate osteochondral repair.

Due to its intrinsic properties, much research on bone tissue engineering has been conducted using PLA. This synthetic polymer is biocompatible and biodegradable, deriving from a natural organic acid, lactic acid (Fig. 2 H) [77]. Since lactic acid can be found as L or D isomer, PLA can be mentioned as poly (L-lactic acid) (PLLA), poly (D-lactic acid) (PDLA), or poly (D, L-lactic acid) (PDLLA). Nevertheless, it is essential to mention that the most common form of lactic acid obtained from biological sources is L-isomers. Considering these features, PLA has been studied, envisioning diverse tissue engineering and regenerative approaches [78,79]. One example is the work of Oliveira et al. [80], where the authors produced a PLA scaffold coated with carbon nanotubes, carbon nanoribbons, and nHA, envisioning the promotion of bone tissue regeneration. An osteopenia animal model was used to assess the effect of the produced scaffold on the promotion of bone regeneration. The data showed that the scaffold was biocompatible and favored osteointegration.

Finally, PCL has been widely used in load-bearing strategies (Fig. 2 I) [38,81]. Despite being biocompatible and biodegradable, this polymer is also hydrophobic hindering cell adhesion. To overcome this disadvantage, it needs further modifications to enhance its bioactivity, as pursued by Stastna et al. [82]. In this work, fibers of PCL and HAp were produced and then treated with low-temperature argon discharge plasma. With this strategy, the authors wanted to improve cell proliferation by adding HAp and improving the wettability of the fibers. It was observed that the addition of HAp increased the proliferation of cells by 10%. In comparison, the conjugation of HAp and plasma treatment increased cell proliferation by 30% compared with the control. In a different example, PCL mixed with HAp was modified with polydopamine, which had two growth factors, BMP-2 and vascular endothelial growth factor (VEGF), to improve the osteoinductivity [13]. The results showed that the developed scaffold presented a superior osteogenic activity.

2.1.3. Ceramics

Bioceramics, such as calcium phosphate and bone cement present a high compressive modulus and can be modified to deliver bioactive ions [83]. Nevertheless, these inorganic biomaterials are usually very brittle, hindering their wider use [84]. Bioceramics can be divided into three main categories, i) ceramics, ii) glasses and iii) glass-ceramics. Regarding their structure, ceramics are crystalline, glasses are amorphous, and glass ceramics are partially crystalline [83,84]. Moreover, bioceramics can be inert or bioactive, depending on their capacity to interact with the surrounding bone tissue environment. As described for biopolymers, bioceramics can also be modified to improve their bioactivity. For example, they can be modified with bioactive ions such as strontium (Sr), zinc (Zn), and manganese (Mn), as described by Pina et al. [85]. This work modified calcium phosphate with these ions to enhance the scaffold's osteogenic properties, envisioning its application in bone tissue engineering. In addition, it was noticed that, while scaffolds containing Zn enhanced cell proliferation, scaffolds containing Sr or Mn improved osteogenic potential, as demonstrated by the increase of ALP activity. Additionally, a combinatory effect was observed upon the mixture of Sr and Zn, as shown by the increase of cell proliferation and osteogenesis.

Calcium phosphates are the most recurrent ceramics used in bone tissue engineering strategies due to their similarities to bone HAp [86–88]. Among those, HAp, tricalcium phosphate (TCP), and the mixture of both, biphasic calcium phosphate, have been standing out (Figs. 2 J–L) [89].

HAp is very similar to the mineral phase of bone tissue, which explains its wide use in bone tissue engineering approaches (Fig. 2 J) [90]. This ceramic presents a ratio of calcium and phosphate of 1.67, is very stable, and presents a low solubility [91]. Furthermore, pure HAp can act as a nucleating site, improving the precipitation of apatite derived from the calcium and phosphate found within the cell culture medium, resulting in an osteoconductive material, but not osteoinductive. Further modifications can be pursued to overcome this issue as the combination with polymers or modified with active ions [92–94].

Considering TCP, the ratio between calcium and phosphate is 1.5 and is more soluble than HAp (Fig. 2 K) [91]. This ceramic presents two different phases, α, and β that, despite having similar chemistry, presents different crystal structures. Moreover, β-TCP is less soluble than α-TCP, which is associated with its osteoconductive and osteoinductive features, motivating researchers to pursue the use of β-TCP for bone regeneration strategies [86,95]. Different combinations of β-TCP can be found in the literature. It can be doped with bioactive ions or combined with biopolymers to improve bone regeneration properties [96,97]. Scaffolds of β-TCP doped with SiO_2 and ZnO showed a slower degradation rate and enhanced bone regeneration than pure β-TCP scaffolds [96]. Considering the combination with biopolymers, it has been demonstrated that collagen-β-TCP composite scaffolds showed enhanced bone regeneration compared with only collagen-based scaffolds [97].

Biphasic calcium phosphates are ceramics with two phases, possessing osteoconductivity similar to apatite and osteoinductivity similar to TCP (Fig. 2 L) [98,99]. They can be obtained by combining HAp with TCP or by producing an apatite deficient in calcium. Depending on the combination and on each phase, different features can be achieved. In this case, the ratio between calcium and phosphate is usually between HAp (1.67) or TCP (1.5). The implantation of biphasic calcium phosphates has been shown to allow the formation of new bone tissue [99]. Additionally, it has been shown that biphasic calcium phosphates can be strong candidates in osteoporosis treatment since it was demonstrated that they could inhibit osteoclast differentiation while favoring the differentiation of osteoblasts [100].

2.1.4. Composites

One strategy to overcome the disadvantage of the different biomaterials (*e.g.*, poor mechanical performance) consists of combining two or more by blending or producing composites. Moreover, considering that bone tissue is a composite that results from the combination of a biopolymer and a ceramic, it is easy to understand the promising tool that a composite can become. In this context, the composites often reported in the literature comprise the mixture of a biodegradable polymer and small particles, commonly ceramics used to improve the mechanical properties of the matrix (biopolymer) [101]. Nevertheless, it is also possible to develop a composite by promoting *in situ* precipitation of HAp [102]. In addition, composites can be developed for locally deliver bioactive molecules, ions, or drugs, depending on the degradation rate of the composite and its porosity [103–106]. Considering the use of composites, the dispersion of ceramics is of most importance to emulate the targeted tissue as much as possible. Envisioning the mimic of bone tissue, it is expected that ceramics are homogeneously dispersed and distributed throughout the polymeric matrix. Moreover, when the objective is to mimic the osteochondral tissue, it is expected to have a gradient of the ceramic concentration throughout the polymer [107]. For example, Xu et al. [108] developed a bilayer composite scaffold for osteochondral repair. In this study, researchers produced a bi-layer scaffold by combining a layer of chitosan and another layer of chitosan with β-TCP. Besides the differences observed at the microstructure level, the authors also concluded that the chitosan layer enables the culture of chondrocytes. In contrast, the layer composed of chitosan with β-TCP supported the culture of osteoblasts. Moreover, upon implantation, the newly formed tissues observed were analogous to the surrounding native cartilage and subchondral bone. Noteworthy, composite biomaterials can also be used in a different scenario than bone tissue engineering and regeneration. By integrating nanoparticles into the composites' formulation, such as magnetic nanoparticles, these biomaterials can be applied as a treatment for bone cancer. For example, a composite of chitosan, hyaluronic acid, collagen, calcium phosphate, and magnetic nanoparticles was evaluated as a strategy to fight cancer [109]. The main goal was to implant the developed composite into the defect site, created upon resection of the tumor, and submit the patient to X-rays to magnetize the nanoparticles, providing a radiotherapy approach. Additionally, the authors included a second step of treatment, consisting in the addition of a chemotherapeutic drug to the magnetic nanoparticles to provide a dual therapeutic strategy.

2.2. Scaffold fabrication strategies

Besides the importance of using the right biomaterial for scaffolds' preparation, another critical step relies on the strategy chosen to fabricate such scaffolds [110]. Depending on the fabrication method, different properties may be obtained, such as different porosities, mechanical properties, and compositional gradients, all crucial properties for mimicry of bone tissue. To choose a suitable fabrication strategy, it is essential to consider the intended architecture and how processing methods will affect the biomaterial selected. From solvent casting to freeze-drying, diverse techniques have been pursued to produce porous scaffolds [110]. Nevertheless, most of those techniques do not allow precise control over the scaffold's architecture, including pore size, pore geometry, distribution, or even interconnectivity, hindering the scale-up of such strategies. Additive manufacturing strategies, namely three-dimensional (3D) printing, stereolithography, fused deposition modeling, and selective laser sintering, enable to outshine classical strategies by producing complex scaffolds in a more precise and reproducible way (Fig. 3).

2.2.1. 3D Printing strategies

Nowadays, one of the most pursued strategies for scaffolds' fabrication is 3D printing [111,112]. 3D printing can be divided into different techniques, such as extrusion, inkjet, and laser-assisted printing (Fig. 3 A). These techniques enable the production of more intricate and reproducible scaffolds *via* a layer-by-layer process. Furthermore, the obtained scaffolds can recapitulate the environmental features of bone tissue with high precision since different biomaterials, growth factors, and cells [113] can be printed simultaneously (3D bioprinting) with precise control over their distribution. Thus, it is possible to produce a patient's-specific scaffold within small amounts of time and cost [114,115]. To create a proper 3D printed scaffold, selecting the most appropriate biomaterial (ink) and the most suitable printing method is essential.

2.2.1.1. Extrusion printing. Extrusion printing has been used worldwide to develop precise structures due to its easy access, flexibility, and affordability [116]. This technique consists of temperature-controlled material handling that allows printing different size structures using computer-aided design (CAD) files. The material is extruded from cartridges by applying a pneumatic force or a mechanical force (Fig. 3 A). Regarding pneumatic force, pressurized air is used to extrude the material. In contrast, in mechanical force, piston or auger screws are used to force the material directly. The choice of each mechanism of extraction relies on the viscoelastic properties of the material to be extruded. For materials with viscosity values between 30 mPa·s and 6×10^7 mPa·s, pneumatic extrusion force is usually used [117]. In comparison,

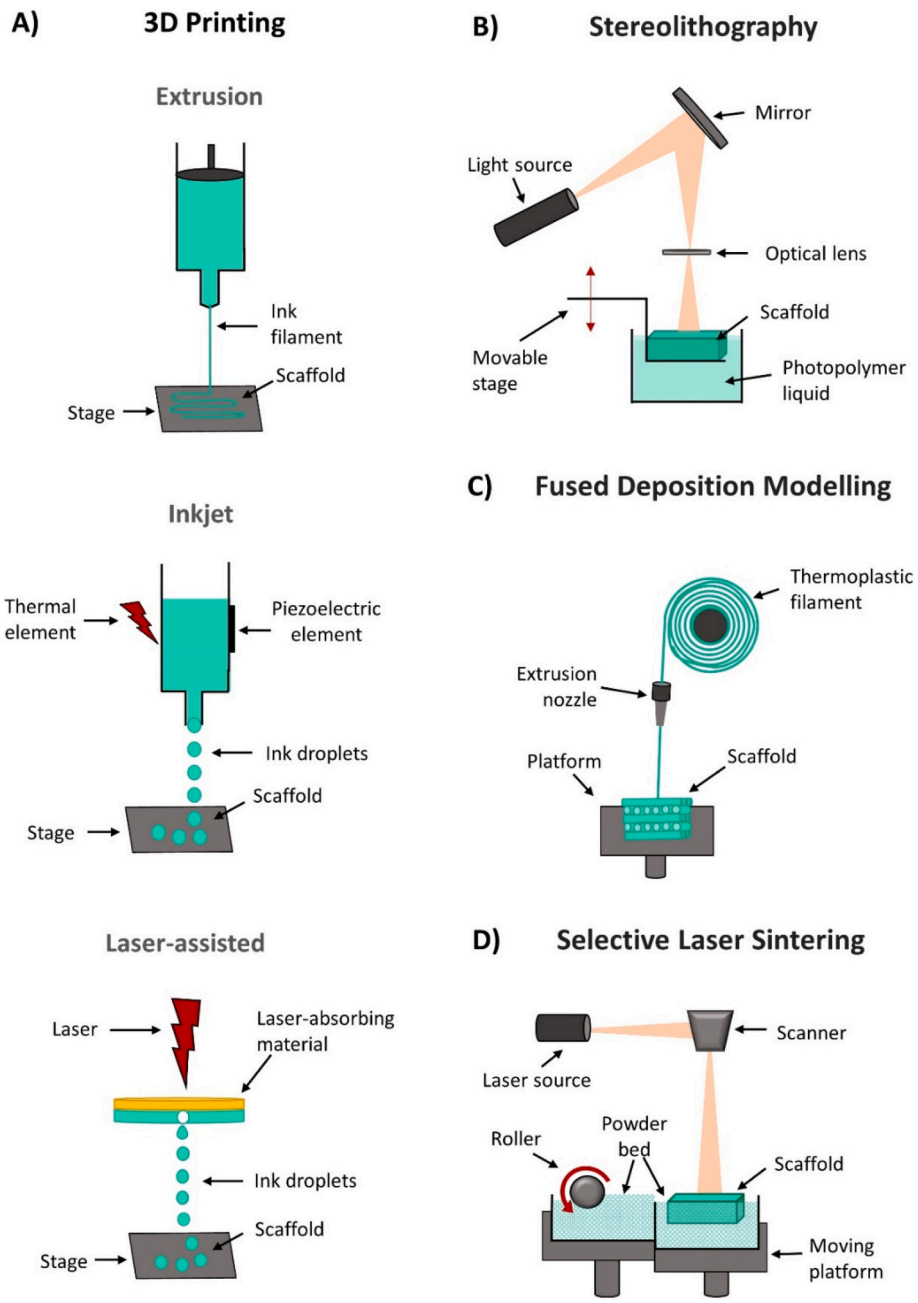

Fig. 3. Schematic representation of additive manufacturing strategies. A) 3D printing strategies: Extrusion, Inkjet and Laser-assisted printing strategies; B) Stereolithography strategy; C) Fused Deposition Modeling strategy; and D) Selective Laser Sintering strategy.

mechanical extrusion force is adequate for viscosity values superior to 6 $\times 10^7$ mPa·s. Due to this versatility, it is possible to print using ceramic-based inks, creating green bodies that give place to ceramic-based scaffolds [118]. Nevertheless, this technique presents three significant drawbacks, namely i) its printing speed, which ranges between 10 and 50 μm/s, ii) its resolution, which is commonly higher than 100 μm, and iii) shear-induced cell death [119]. Despite these drawbacks, extrusion printing is being widely used in bone tissue engineering approaches. For example, this technique enabled the development of constructs capable of mimicking the bone tissue microstructure and including a perfusable vascular lumen [120].

2.2.1.2. Inkjet printing. Inkjet printing is a high-resolution technique that dispenses precise droplets of bioink within the picolitre's range using thermal and piezoelectric approaches (Fig. 3 A) [121]. In both cases, the droplets can be deposited into two modes: i) in a continuous with a printing speed of >10 m·s^{-1} or ii) in a drop-on-demand way with a printing speed of 5–8 m·s^{-1} [112,122,123]. The resolution of continuous deposition is 100 μm and of drop-on-demand deposition is 20–50 μm [124]. Nevertheless, the most common approach is based on temperature (thermal approach) since it renders the higher cell viability rates, is easy to use, and presents lower associated costs [122]. In the thermal approach, air bubbles are created upon an increase of the temperature of the print head, which then collapses, generating pressure pulses that eject the bioink droplets. Several droplets' volumes can be printed, depending on temperature gradient, frequency of the pulse, and bioink viscosity. In the piezoelectric approach, the droplets are formed due to applying a current to the piezoelectric elements present [125]. These elements distort or expand with the current, forcing the creation of a drop throughput of the nozzle, which can vary in volume. One of the

main drawbacks of inkjet printing is the difficulty of using high viscous bioinks since it can clog the needle, exposing cells to high shear forces, resulting in cell death. For this reason, the most suitable bioinks to be used by this method must present low viscosity (20–40 mPa·s) [126].

Inkjet bioprinting has been a promising approach to producing bone tissue models with high spatial resolution. It allows a uniform and highly specific disposition of cells [127]. Moreover, it can be combined with other processing techniques for the creation of more relevant models. For example, in the case of 3D bioprinted *in vitro* models of bone and cartilage, one of the main weaknesses is the mechanical properties of the bioinks used [128]. Usually, these bioinks presents mechanical properties lower than the native tissue, hindering the success of developed approaches. Nonetheless, inkjet bioprinting in a more advanced fabrication stage made it possible to homogeneously distribute MSCs in a more mechanically relevant scaffold [129]. Printed cells showed high survival rates and, upon analysis of gene and protein expression, were found to be differentiating along the osteogenic and chondrogenic lineage. In a different study, several human trabecular bones (femoral head, proximal tibia, and vertebral body) were scanned by micro-CT [130]. Their morphometric properties were used to develop bone-like constructs composed of reactive polyurethane-hydroxyapatite. The resulted hybrid comprised amounts of hydroxyapatite (>50%) within the range found in bone (50–70 wt%). Also, it mimicked the mechanical properties of the different human trabecular bones, such as the femoral head, proximal tibia, and vertebral body. These similarities showed to be an essential feature for osteoblast differentiation and mineralization. Also, it was demonstrated that the different morphometric properties mimicked, influenced cell differentiation. Less convex surfaces (emulating femoral heads) promoted higher osteoblast differentiation and mineralization than predominately convex surfaces (simulating proximal tibia and vertebral femur). In this reasoning, the authors demonstrated the importance of mimicking patients' bone tissue in treating skeleton diseases.

2.2.1.3. Laser-assisted printing. Laser-assisted allows printing with high precision and micrometer resolution (≈10 μm) [131–133]. The technique relies on a laser-induced deposition of cells and/or biomaterials (Fig. 3 A). Briefly, it comprises an energized pulsed laser, a ribbon containing the biomaterial, and a stage where the biomaterial will be printed. The ribbon containing the biomaterial is usually composed of a transparent substrate (*e.g.*, glass) that is coated with a layer of laser-absorbing metal (*e.g.*, gold) and with the biomaterial deposited on top. The laser beam vaporizes the metal layer, transferring droplets of the biomaterial onto the substrate. These steps influence printing resolution, namely the thickness of the ribbon layer, the biomaterial's mechanical properties, the laser pulse's energy, and the printing speed that can reach 100 $m{\cdot}s^{-1}$ [132,133]. This unique technique has the advantage of being nozzle-free, allowing to print biomaterials with a viscosity ranging from 1 to 300 mPa·s [131]. It enables the printing of tiny droplets with high cell densities (≈10^8 cells/mL). Nevertheless, some studies have shown that laser irradiation can damage cells, diminishing their viability [131,134]. Another concern relies on the limited availability of photocurable biomaterials.

Despite these disadvantages, this technique has been successfully used to develop improved strategies for tissue regeneration. For example, Keriquel et al. [135] bioprinted MSCs, collagen, and nHA for bone tissue regeneration. In this study, first, cells were bioprinted in a collagen matrix with different arrangements, ring, and disk arrangements. In opposite to other studies, no harmful effect on cells' viability was observed using laser-assisted bioprinting. Interestingly, as proof of concept, the authors bioprinted *in situ* in a mice calvaria defect the different cellular arrangements within two disks of collagen with nHA. New bone formation was observed in bioprinted disk format, while in the ring format or solely collagen with nHA disks, scarce new bone formation was observed. In a different study, laser-assisted bioprinting was used to print single cells precisely to produce a more physiological-relevant bone tissue model [136]. This technique enabled the authors to position endothelial cells into bone-like cell sheets, which seven days post-printing were able to reorganize and form tubule-like structures. Moreover, no harmful effect on cell viability was observed.

2.2.2. Stereolithography

Stereolithography is based on the polymerization of photosensitive materials (with a maximum viscosity of 5 Pa·s) in a platform immersed in a photopolymer liquid, enabling the polymerization of the layer exposed to light. In contrast, the no exposed layer does not polymerize (Fig. 3 B) [137–140]. By repeating the downwards movement of the stage, it is possible to produce a 3D scaffold layer-by-layer at speed as high as 100 $\mu m{\cdot}s^{-1}$ [141]. In the end, the non-polymerized material is removed. This technique is the one that enables the highest resolution as compared with other additive manufacturing techniques (≈50 μm) [142]. To allow the printing of cells by this technique, some details must be considered, as the type of light used to polymerize the biomaterial. For example, Lin et al. [24] developed a live-cell fabrication technology allowing printing 3D structures with cells by stereolithography using visible light. With this technique, the authors guaranteed that cells were viable and distributed along the scaffold. Moreover, upon induction with BMP-2, it was observed that entrapped cells were able to differentiate along the osteoblastic lineage *in vitro* and to form new bone in *in vivo* studies.

2.2.3. Fused deposition modeling

Fused deposition modeling is a technique that comprises prefabricated filaments of thermoplastic polymers (*e.g.*, PCL or PLGA). Upon heating, thermoplastic polymers can be extruded at a printing speed of ≈200 $m{\cdot}s^{-1}$ and a resolution of 300 μm from a nozzle creating 3D porous scaffolds layer-by-layer on a platform (Fig. 3 C) [137,143–145]. Besides thermoplasticity, the biopolymers should also possess a suitable viscosity and suitable melting and solidification features. PCL is one example of a biocompatible and biodegradable polymer that has been successfully used. It has been approved by the US Food and Drug Administration (FDA) to develop a commercial 3D scaffold obtained upon fused deposition modeling, such as Osteoplug™ (Osteopore® – Singapore) [146]. Nevertheless, to improve the properties of PCL scaffolds and increase the similarity with bone tissue, it has been combined with ceramics (*e.g.*, HAp), as reported by Jiao et al. [143]. In a different example, PCL scaffolds have been coated with cell-derived extracellular matrices [147]. The addition of the matrix to PCL scaffolds enhanced the adhesion and proliferation of stem cells, ultimately improving their osteoinductive properties.

2.2.4. Selective laser sintering

Selective laser sintering is a technique that produces 3D scaffolds by melting powders using high-powered CO_2 or Nd:YAG lasers (Fig. 3 D) [137]. In this sense, a wide variety of biomaterials ranging from PCL to ceramics can be used, resulting in a resolution of ≈200 μm [137]. To produce a 3D scaffold, layer by layer of powder is placed and exposed to the laser merging accordingly with the wanted design at a speed of ≈200 $m{\cdot}s^{-1}$ [148]. In the end, the remained powder not merged is discarded. Tan and co-workers used this technique to produce scaffolds of PLLA, HAp, and metformin [149]. The fabricated scaffold presented good mechanical strength provided by PLLA, bioactivity provided by HAp, and antitumor properties provided by metformin. Moreover, the results have shown that the scaffolds produced by this approach enabled bone regeneration and inhibited tumor formation, demonstrating that they can be a powerful tool in treating tumor-induced bone defects.

One of the main drawbacks of this technique relies on the high operating temperatures necessary for scaffold production, which may damage materials' properties and reduce their mechanical properties [137]. For so, approaches to improve the features of scaffolds produced by selective laser sintering have been investigated. For example,

scaffolds have been mixed with microparticles of sodium chloride and then re-melted and re-solidified, which enhanced the mechanical properties of the developed scaffold [150].

Noteworthy, the development of printed 3D constructs that can alter their form upon external stimuli, termed four-dimensional (4D) printing, has become more appealing, including in bone tissue engineering [151]. It is still a challenge to implant a scaffold due to the uneven form of the defect. Thus, using the 4D printing approach, a scaffold can be produced resembling the complex biological environment of bone and further implanted into any site, adapting closely to the defect. Photothermal responsive biomaterials are attractive candidates for this type of approach, as described by Wang and colleagues [152]. In this study, the authors reported producing a composite scaffold composed of black phosphorus nanosheets and osteogenic peptide into β-TCP mixed with poly (lactic acid-*co*-trimethylene carbonate). Moreover, the authors demonstrated that, after its production, the application of irradiation and increasing temperature promoted the reconfiguration of the scaffold. This behavior allowed that, after implantation, the scaffold was precisely confined within the bone defect, enabling new bone formation. Despite the promising results of this approach, favoring a surgical scenario for its easy and fast use, the availability of such biomaterials is still minimal.

3. Biomimetic scaffold-free strategies

Scaffold-free strategies have also been widely pursued for tissue engineering approaches [153]. In the case of scaffold-based strategies, the researchers mainly search for the application of osteoconductive/osteoinductive scaffolds and osteogenic cells mimicking the intramembranous ossification process, where there is a direct formation of bone tissue [154]. While, in the case of scaffold-free strategies, they mainly envision the simulation of the embryological process of endochondral ossification, characterized by a remodeling of a hypertrophic cartilaginous template into bone [155,156]. In addition, it is essential to point out that despite the majority of scaffold-based studies aim to mimic the intramembranous ossification process, some seek to emulate endochondral ossification [157–159].

To mimic endochondral ossification, the development of cartilaginous tissue using tissue engineering strategies has been investigated, foreseeing replacing the engineered cartilage with new bone [155,160]. Scotti and colleagues developed an engineered cartilage approach to induce bone formation [161]. In more detail, researchers developed early hypertrophic and late hypertrophic tissues inside of transwells and implanted them subcutaneously in nude mice. The results showed that late hypertrophic tissues were capable of generating *de novo* bone tissue. In a different strategy, induced pluripotent stem cells were induced towards chondrogenic lineage, producing cartilaginous pellets that regenerated vascularized bone tissue *via* endochondral ossification *in vivo* [160]. Nevertheless, despite these promising results, studies have indicated different bone regeneration rates depending on donor cells' capacity to differentiate into chondrogenic lineage [162]. One drawback of using cellular pellets is the possibility of forming necrosis areas in the pellet's core, hindering the approach's success. The use of fewer cells has emerged as an easy way to circumvent that issue, avoiding bioreactors. Remarkably, the use of fewer cells resulted in the enhancement of chondrogenic differentiation [163]. In a different approach, aggregates of stem cells were condensed to induce endochondral bone formation *in vivo* [164]. In this approach, stem cell sheets were prepared and condensed into a cylindrical shape before implantation in a critical-sized bone defect. The results have shown the production of a zonal human cartilage and primary spongiosa, which emulated the native growth plate. Noteworthy, in this study, the devitalization of the condensed sheets hindered the formation of bone. Moreover, mechanical loading promoted by internal fixation plates with different stiffness improved cell condensation and induced endochondral ossification.

In a different study, microspheroids of periosteum cells were used to produce a callus organoid emulating the establishment of soft callus during fracture healing [165]. The developed organoids could form a large tissue by bio-assembling *in vitro*, favoring the regeneration of bone defects *in vivo*. The regeneration of bone defects occurred within the timeline of natural healing, and the resultant structure was similar to the native long bone. Furthermore, the successful healing of bone tissue by assembling cell spheroids into bigger structures showed improved results compared with common macro-scale approaches, which may transform the field of bone tissue engineering.

Even so, the approaches above face some critical issues regarding scalability, namely concerning vascularization. Without a proper flow of nutrients and cellular waste, bigger structures will present necrotic cores, similar to big cellular pellets as previously stated, hindering the success of such approaches.

3.1. Biofabrication Strategies

Considering the fabrication techniques used in scaffold-free strategies, bioprinting has emerged as a powerful tool to obtain scaffold-free structures. Despite, the most common approach is the printing of bioinks, *i.e.*, a cell suspension mixed with ink [166], new approaches have been developed to cell aggregates deposition, such as cell spheroids, envisioning the achievement of organ-like structures [167,168]. In this sense, the aggregates can be bioprinted in a controlled manner, working as building blocks of tissue- or organ-like structures. Such strategies may rise scaffold-free strategies used for endochondral ossification into a new dimension.

Different bioprinting strategies have been pursued in bone tissue engineering as bioprinting in supporting baths, aspiration-assisted bioprinting, microtissue singularization bioprinting, and the Kenzan method.

3.1.1. Bioprinting in supporting baths

Bioprinting in supporting baths is a technique developed to print precise structures using bioinks with low mechanical properties [169]. For this, bioinks are extruded omnidirectional, contrary to typical layer-by-layer deposition, into a bath, becoming suspended, which prevents its collapse. For so, a new range of opportunities that enable a higher level of mimicry, producing structures with less cell constraint, becomes available. The suspension bath is commonly composed of yield stress materials that support the suspension of the structure and completely surround the structure. In this sense, the materials of the supporting bath typically present a solid-like nature that, after applying stress, became liquid-like, and upon removal of stress, became solid-like again [170]. Suspension baths are mainly condensed microgel systems. One example is the gellan fluid gels, which are condensed dispersions of gellan microparticles [170]. Gellan fluid gels become liquid-like as an extrusion tip travels within the gel to print the ink, distorting the microgels. Then, the microgels become solid-like as the tip moves away, entrapping the printed structure. Finally, upon polymerization of the printed structure that in this case can be obtained upon enzymatic, thermal, ionic, or photoinitiated cross-linking processes, the gellan fluid gels are washed away.

This technique has been used to develop scaffold-free bone and cartilage engineering strategies [171]. In this approach, human stem cells were printed within a suspension bath composed of oxidized and methacrylated alginate that, upon ionic crosslink, enabled the printing of cells and, upon photocrosslinking, enabled long-term culture. The results showed that cells could aggregate and differentiate along bone and cartilage lineage since the supporting bath favored the flow of nutrients and induction growth factors.

3.1.2. Aspiration-assisted bioprinting

The bioprinting of spheroids in a 3D organized structure has been a challenge since spheroids can aggregate inside the nozzle clogging it or can disassociate, losing their format [168,172]. A new technique was

developed to overcome these challenges, named aspiration-assisted bioprinting [167,173]. This technique allows the precise positioning of spheroids with different sizes, ranging from 80 to 800 μm, within a hydrogel using minimal picking and lifting aspiration forces, resulting in insignificant cellular damage. Indeed, aspiration-assisted bioprinting was used to print spheroids of MSCs and hUVECs after 10 days of osteogenic induction to produce a bone tissue-like structure [167]. Besides the precise positioning of the co-cultured spheroids, the authors also observed no relevant alterations in the shape of the spheroid. Moreover, the printed bone tissue-like structures showed interconnecting with each other and expressing osteogenic and endothelial genes. In a different work from the same group, it was observed that by submitting the cell's spheroids to different osteogenic induction time-frames, it was possible to control the format of the printed spheroids [173]. Moreover, using this approach, consistent mineral deposits were detected. Interestingly, no differences in gene expression were observed. A different study reported the production of osteochondral tissues using this technique (Fig. 4) [174]. For that, spheroids of ASCs were obtained and induced into the osteogenic and chondrogenic lineage. Later, the two sets of spheroids were positioned into a sacrificial hydrogel by bioprinting a layer of chondrogenic spheroids on top of the other layer of osteogenic spheroids. The results showed that each layer of spheroids could interconnect, maintain their phenotype, and emulate a native osteochondral tissue.

3.1.3. *Microtissue singularisation bioprinting*

The singularization technique comprises the individualization of spheroids and microtissues (≈1.1 mm of diameter) with an efficiency of 97% and without damaging the cells, enabling the positioning of each one on demand [175]. For that, by altering the hydrodynamic forces that the microtissues are subject to and associate them with hydraulic valves, it is possible to select and trap singular microtissues that are then delivered to an injection system. Upon this point, the microtissue can be bioassembled into a previously developed structure, creating a bioassembled hybrid construct. This technique can be a powerful tool to produce hierarchical bioassembled co-cultures or tissues. In an attempt to produce an osteochondral biphasic model for joint resurfacing, a semicircular structure was created, and individual microtissues of chondrocytes were bioassembled within the structure [175]. The authors observed an enhancement of biomarkers of hyaline cartilage, namely glycosaminoglycans and collagen type II. Moreover, microtissues were able to interconnect, secreting extracellular components without creating necrotic regions nor dedifferentiating.

3.1.4. *Kenzan method*

Kenzan method is based on the use of micro-needles (Fig. 5) [168,176]. In this approach, cell spheroids are developed (Figs. 5 A–B), transported by a mobile nozzle arm, and immobilized into a microneedle array that acts as temporary support (Figs. 5 C–H). The needles are at a distance of ≈500 μm, which favors the interconnection of spheroids and consequently the secretion of extracellular matrix, enabling the large-scale assembling of spheroids into multiple layers. Moreover, since the spheroids are placed at a regular distance, the perfusion of nutrients is facilitated. Yamasaki et al. [177] used this method to develop a tubular construct of spheroids of ASCs, to regenerate osteochondral defects (Fig. 5). Tubular constructs were first cultured for 7 days to produce an extracellular matrix. The created extracellular matrix was composed mainly of collagen type I, which increased the tubular constructs' strength and elasticity (Figs. 5 E–H). Two different tubular sizes were obtained to implant the smaller tube within the larger tube to fill the osteochondral knee defect (Figs. 5 I–M). Upon implantation, the results indicated that the constructs favor the

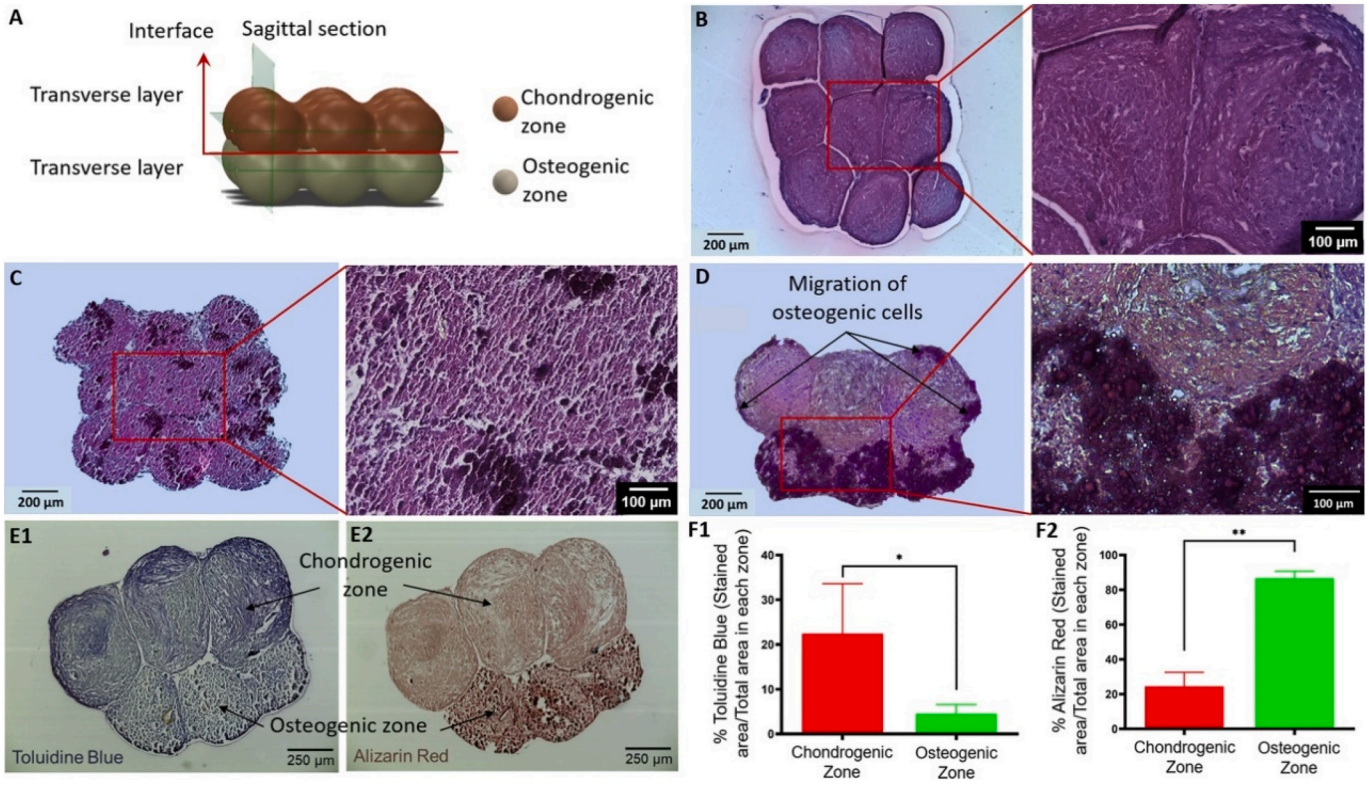

Fig. 4. Production of osteochondral tissues using aspiration-assisted bioprinting. A) Schematic representation of osteochondral construct composed of one layer of osteogenic spheroids and a second layer of chondrogenic spheroids; (B—D) Osteochondral construct stained with Hematoxylin and Eosin showing the chondrogenic and osteogenic regions, and the interface; (E1-E2) Osteochondral construct stained with Toluidine Blue and Alizarin Red stainings showing the chondrogenic or osteogenic regions; and (F1-F2) Quantification of the stained regions for Toluidine Blue and Alizarin Red. Reprinted with permission from [174] under Creative Commons Attribution License.

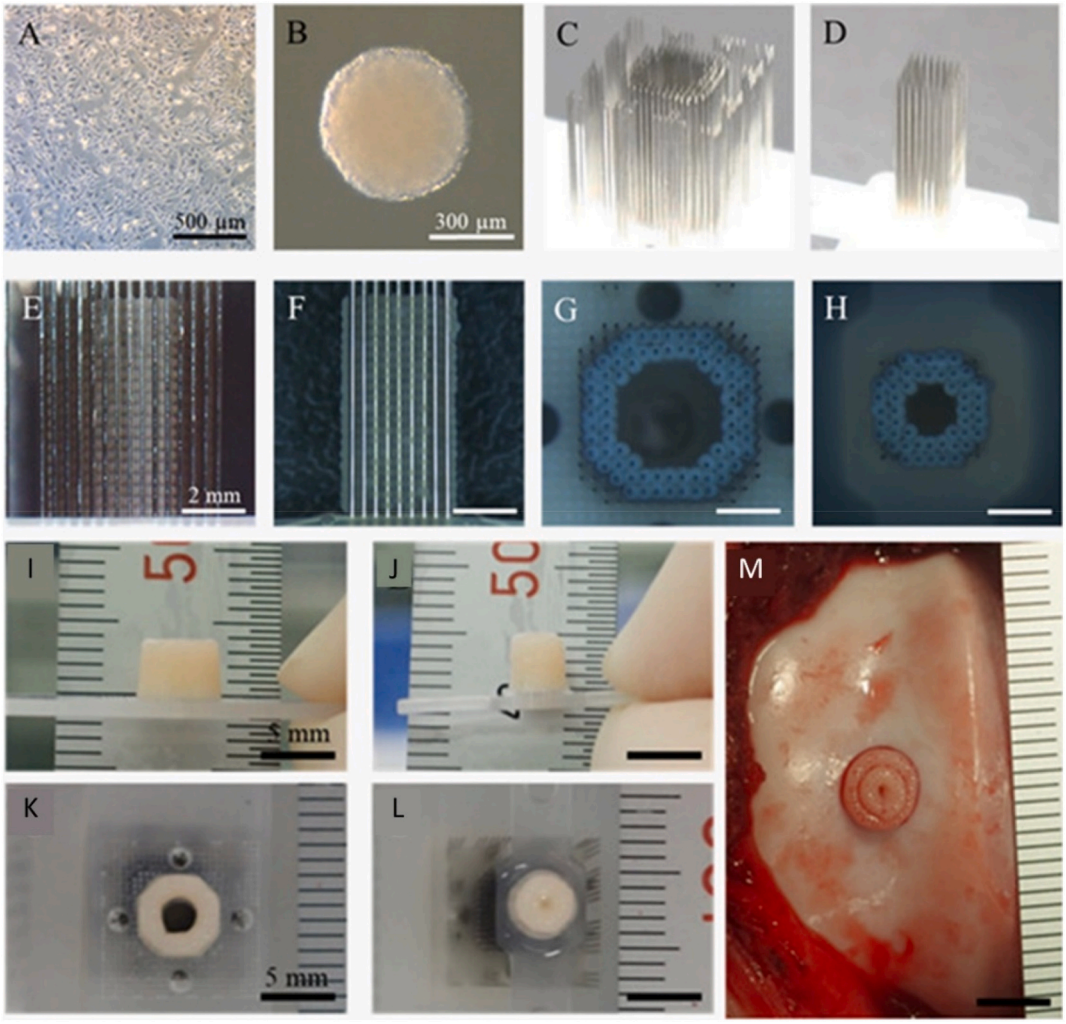

Fig. 5. Spheroid-based constructs produced using the Kenzan method. A) ASCs in culture to produce cell spheroids; B) Spheroids of ASCs; C) Large needle-array; D) Small needle-array; E–F) Lateral view of spheroid immobilized into the large needle-array (E) and the small needle-array (F); G–H) Top view of spheroid immobilized into the large needle-array (G) and the small needle-array (H); I–J) Lateral view of large (I) and small (J) spheroid-based constructs; K–L) Top view of large (K) and small (L) spheroid-based constructs; and M) Grafting of the smaller construct within the larger construct to fill the osteochondral knee defect. Adapted with permission from [177] © 2018 Orthopaedic Research Society. Published by Wiley Periodicals, Inc.

formation of subchondral bone.

In a different study, this method was used to develop constructs to be implanted into defects in human osteoarthritic cartilage explants and subchondral defects in rabbits [178]. For the first construct, the authors used human infrapatellar fat pad MSCs, and for the second construct, authors explored the use of human embryonic-derived MSCs. In both cases, constructs were allowed to secret extracellular matrix and merge before implantation, being the time of maturation 4 days for infrapatellar fat pad MSCs constructs and 5 days for embryonic-derived MSCs constructs. Upon three weeks of implantation into osteoarthritic tissue defects, infrapatellar fat pad MSCs construct formed neocartilage tissue, which was integrated into the host tissue. At the same time, not implanted constructs were used as control, and the results showed that they developed into a mixture of hyaline-like cartilage and fibrocartilage. Considering the embryonic-derived mesenchymal stem cell constructs, they were implanted for 8 weeks into rabbit osteochondral defects. After this implantation period, matured neotissue was observed fully integrated into the surrounding cartilage and subchondral bone. As in the first construct, this construct was also cultured *in vitro* as a control, mainly showing the development of fibrocartilage.

4. Biomimetic vascularized strategies

Bone tissue presents an extensive vascular network that bone tissue-engineered approaches have been struggling to mimic by using pre-vascularized scaffolds or pre-vascularized cellular aggregates (Fig. 6) [26,179].

Despite the known fact that nutrients' exchange between cells and capillaries is restricted to a distance that can vary between 100 and 300 μm, the development of approaches comprising microvascularization is still a challenge [150]. Also, bone tissue-engineered strategies lack larger vessels to guarantee the perfusion of blood flow along with the graft. Both scales of vascular vessels are essential for the success of osteogenesis and osteointegration until reach functional bone tissue. In the absence of a vascular network, the integration of implanted grafts with the host can fail, and the graft's core can become necrotic. Thus, it is crucial to include within the bone engineering strategy features that induce vascularization. Some strategies included the delivery of bioactive agents to promote angiogenesis [182,183], but the ingrowth of vascular structures is most often slow, resulting in the failure of the bone graft.

With this in mind, different approaches have been pursued to develop more efficient pre-vascularized scaffolds or pre-vascularized

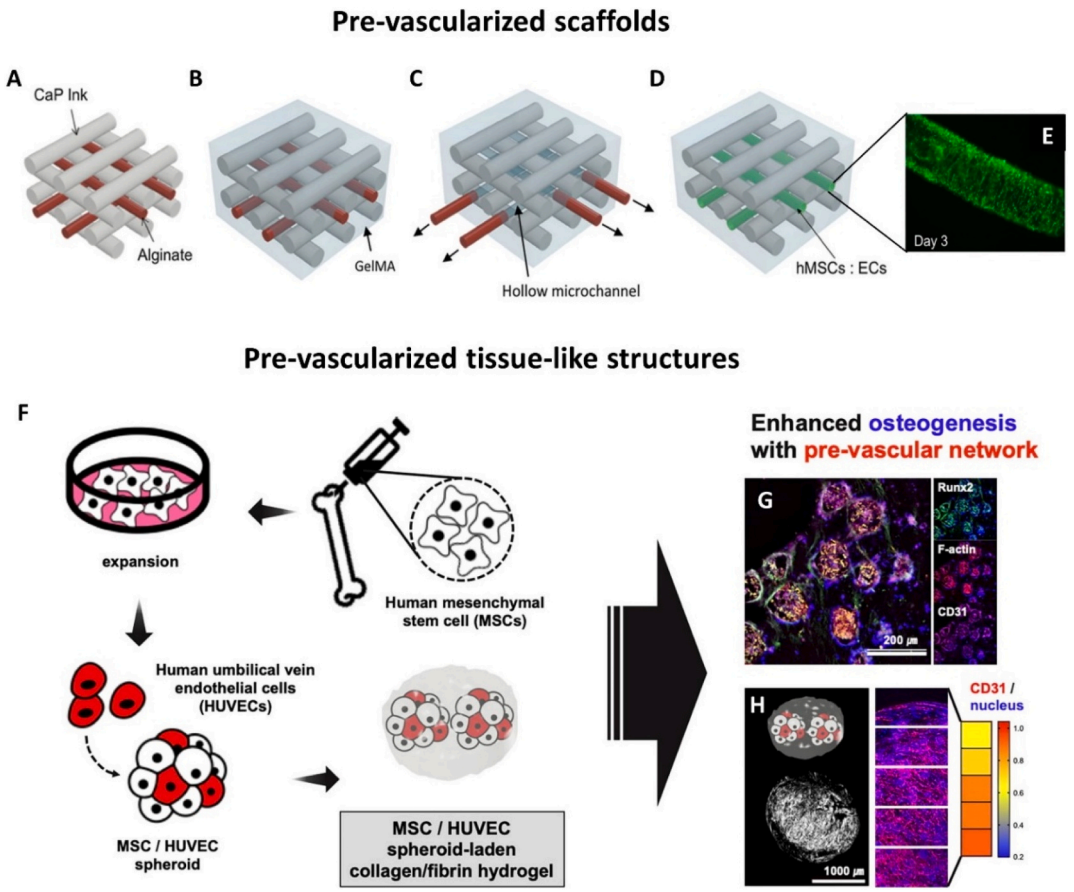

Fig. 6. Development of pre-vascularized scaffolds and pre-vascularized cellular aggregates. A) 3D printed scaffold of calcium phosphate (CaP) and alginate; B) Printed scaffolds covered with photo-crosslinkable gelatin methacryloyl (GelMA); C) Extraction of alginate filaments after gelatin polymerization to produce empty channels; D) Empty channels seeded with co-cultures of human endothelial cells (EC) and human mesenchymal stem cells (hMSCs); E) Endothelialized channels after 3 days of culture; F) Schematic representation of spheroid-laden hydrogels fabrication. MSCs were isolated, expanded, combined with hUVECs to produce spheroids of MSCs and hUVECs, which were then entrapped within a collagen/fibrin hydrogel; G) Spheroids stained for runt-related transcription factor 2 (RUNX2, green), F-actin (red), and CD31 (purple), showing that osteogenesis was enhanced; and H) Spheroids stained for CD31 (red) and cell nuclei (blue), indicating the presence of a pre-vascular network. Reprinted from [180,181] with permission from Elsevier. (For interpretation of the references to colour in this figure legend, the reader is referred to the web version of this article.)

cellular aggregates, as described in Table 1 [180,181,184–188].

4.1. *Pre-vascularized scaffolds*

The design of scaffolds that included approaches based on the use of cells or biomolecular cues to induce the development of vascular systems has been struggling to control the arrangement of the newly formed vascular network. Strategies to induce vascularization are often reported, but no evident control over the vascular network has been demonstrated [189]. Such control, emulating the native hierarchical vascular network, is essential to guarantee a homogeneous distribution of nutrients and oxygen throughout the engineered tissue. For so, fabrication techniques, such as 3D printing and co-culture techniques, have been pursued to obtain vessel-like structures within engineered pre-vascularized constructs [180,184,185,190]. Currently, 3D printing has enabled more complex pre-vascularized scaffolds, as described by Kuss et al. [184]. In this study, researchers entrapped ASCs and hUVECs within hydrogels of hyaluronic acid and gelatin. Later, cell-laden hydrogels were mixed with 3D printed PCL and HAp composite scaffolds. After three weeks in culture, capillary-like networks were observed inside the 3D printed scaffold, but no significant effects were observed concerning osteogenesis. Upon implantation of the pre-vascularized scaffolds, the authors observed microvessel formation and promotion of anastomosis of vascular networks formed by the human implanted cells. In a different work, an approach focused on fabricating 3D sacrificial templates was studied (Figs. 6 A–D) [180]. For that, filaments of calcium phosphate and alginate were printed (Fig. 6 A) and covered with photo-crosslinkable gelatin methacryloyl (GelMA) (Fig. 6 B). Upon polymerization of gelatin, alginate filaments were extracted, leaving empty channels (Fig. 6 C) that were further colonized with co-cultures of hUVECs and BMSCs (Fig. 6 D). The results demonstrated that the used approach enabled printed pre-vascularized bone scaffolds, which presented endothelialized channels in 3 days (Fig. 6 E). Nevertheless, the production of pre-vascularized scaffolds using sacrificial template approaches results in simple architectures, while native tissues comprised complex architectures. Thus, a different strategy comprising the development of pro-angiogenic environments to accelerate the development of pre-vascularized scaffolds, has been reported by Deng et al. [185]. In this study, porous scaffolds composed of β-TCP e and calcium silicate were produced by 3D printing and seeded with co-cultures of hUVECS and BMSCs. The results showed that the printed scaffolds stimulated the secretion of VEGF by BMSCs, which by itself stimulated angiogenesis *in vitro*. In fact, the authors observed the formation of microcapillary-like structures on scaffolds. Furthermore, in an *in vivo* scenario, the colonized scaffolds showed to accelerate early vascularization and induced ectopic bone formation.

Table 1
Pre-vascularized scaffolds and cellular aggregates strategies.

	Strategies	Cells	Main results	Refs
Pre-vascularized scaffolds	3D printed PCL/HAp scaffolds surrounded by spheroid-laden HAMA/GelMa hydrogel	ASCs hUVECs	- *In vitro* vascularization with the formation of capillary-like networks, cell migration, and sprouting, without significantly affect osteogenesis; - *In vivo* microvessels formation and promotion of anastomosis of vascular networks with both human and mouse origin.	[184]
	Dual-ink 3D printing of sacrificial templates of CaP and Alginate surrounded by GelMA	hUVECs BMSCs	- Endothelial monolayer formation in 3 days and subsequent sprouting *in vitro*.	[180]
	3D printing β-TCP and CS	hUVECs BMSCs	- Stimulated angiogenesis through the formation of microcapillary-like structures and secretion of specific growth factors to recruit BMSCs *in vitro*. - Enhanced early vascularization and ectopic bone formation *in vivo*.	[185]
Pre-vascularized cellular aggregates	Spheroids laden-fibrin hydrogels	hUVECs MSCs	- Vascular network formation after 3 weeks of culture *in vitro*. - Vascular networks rapidly perfused and enhanced vascularization *in vivo*.	[186]
	Spheroid laden-collagen/fibrin hydrogels	hUVECS MSCs	- Enhanced pre-vascular network formation. - Up-regulation of osteogenic differentiation markers and increased bone mineral deposition.	[181]
	Sacrificial writing using gelatin ink, into EBs-laden collagen/Matrigel hydrogels	iPSC-derived EBs	- Development of perfusable cellular aggregates by embedding vascular channels.	[187]
	Bioprinted-assisted tissue emergence into Matrigel/collagen hydrogels	hUVECs	- Production of self-organized branched vascular tubes with a lumen that could be perfused. - Interconnected vascular network upon VEGF induction.	[188]

PCL - poly(ε-caprolactone); HAp - hydroxyapatite; HAMA - methacrylated hyaluronic acid; GelMA methacrylated gelatin; ASCs - adipose-derived mesenchymal stem cells; hUVECs - human umbilical vein endothelial cells; CaP - calcium phosphate; BMSCs - bone marrow mesenchymal stem cells; CS - calcium silicate; iPSCs - induced pluripotent stem cells; EBs - embryoid bodies; VEGF – vascular endothelial growth factor.

4.2. *Pre-vascularized cellular aggregates*

Cellular aggregates have been widely investigated to develop pre-vascularized strategies [181,186,191,192]. Gorkun et al. [191] showed that spheroids comprising solely ASCs present the capacity to spontaneously differentiate along the osteogenic and the angiogenic lineage, contributing to the formation of blood vessel networks within an implanted scaffold. Nevertheless, the authors observed that the expression of osteogenic markers surpassed the levels of angiogenic markers, indicating the development of higher numbers of osteogenic cells, which can compromise the development of efficient vascular networks. To better control the development of vascular structures, co-cultures of cellular spheroids of endothelial and stem cells have been pursued and showed promising results. For example, hUVECs and MSCs spheroids entrapped within a permissive matrix showed to induce the development of vascular networks [186]. After being implanted *in vivo* in a critical size calvarial defect, the implanted network showed to not only endured but also perfused with the host vascular networks, boosting vascularization. Moreover, the implanted pre-vascularized structures promoted early new bone formation. Similar results were observed by Heo et al. [181]. In that study, the authors reported developing a pre-vascular network and enhanced osteogenic differentiation (Figs. 6 F–H). Noteworthy, it was observed that the length of vessel-like structures was higher than when only one type of cells was assessed, indicating the importance of cellular signaling between the two types of spheroids [186]. In fact, upon the combination of bone and endothelial cells, it has been observed an increase in the expression of angiogenic factors, such as VEGF and intercellular adhesion molecule 1 [193]. Such enhancement can promote the proliferation of endothelial cells and the development of tubular-like structures.

Despite the advances achieved using such pre-vascularized high cell-density systems, its organization into larger structures has been constrained by diffusion limitations. New strategies have been developed to overcome such constraints and produce microtissues in a controlled manner and with larger vessels capable of perfusing, such as for sacrificial writing into functional tissue and bioprinted-assisted tissue emergence [187,188].

Sacrificial writing into functional tissue relies on using sacrificial ink to print structures within a bath composed of cellular spheroids immersed in an extracellular matrix solution [187,194]. Skylar-Scott and colleagues [187] developed cellular aggregates with embedded vascular channels using this technique. Researchers produced cellular spheroids of induced pluripotent stem cells and mixed them with a solution of collagen type I and Matrigel at 4 °C. Then, a vascular structure was printed within the previous mixture using gelatin-based ink. Upon increasing the temperature, the collagen type I and Matrigel solution underwent gelation, while the gelatin dissolved, resulting in cellular aggregates with vascular channels embedded. With this approach, researchers were able to connect a pump to perfuse culture media. Interestingly, after 24 h of culture, the spheroids fuse, contracting the matrix, and viable cells were observed within a range of 4 mm of thickness. Furthermore, the authors perfused endothelial cells along with the vascular structures but struggled to obtain complete coverage. Moreover, it is essential to point out that the perfused cells adhered and developed a cobblestone pattern. With these strategies, it was possible to create cerebral and cardiac tissue-like perfusable structures.

Bioprinted-assisted tissue emergence was developed by Brassard et al. [188] to enhance the control over tissue's microarchitecture, envisioning the production of centimeter-scale tissues. For the development of such a technique, the authors combined a bioprinter and a microscope. With this combination, moving the microscope stage made it possible to place multiple types of cells sequentially within specific locations, giving rise to different geometries and cellular arrangements

in real-time by perforating a bath composed of a permissive extracellular matrix. The bath was further polymerized at the end of printing, maintaining the positioning of the cells. With this technique was possible to control the geometry and the cellular density of bioprinted stem cells and organoids, favoring the multicellular organization and creating organized tissues as branched vasculature. In fact, by bioprinting hUVECS, it was possible to produce self-organized branched vascular tubes with a lumen that could be perfused [188]. Moreover, upon their stimulation with VEGF, the formation of capillaries was observed.

5. Conclusions

Bone tissue engineering has been evolving over the years towards addressing the challenges of tissue mimetic requirements. Indeed, an ideal scaffold should emulate a patient's healthy bone tissue to be substituted by functional regenerated tissue in a precise way. To accomplish this goal, different polymeric and ceramic biomaterials have been used from natural and synthetic origins. Although natural-based polymeric biomaterials present some advantages such as comprising cellular adhesion sites and being biodegradable, enabling tissue ingrowth, synthetic polymeric biomaterials offer improved mechanical properties and negligible batch-to-batch variation. Regarding ceramics, since calcium phosphates are very similar to bone HAp, many tissue engineering approaches have been the focus of their study. Nevertheless, they are brittle biomaterials which prompted researchers to find other alternatives. In this sense, polymers and ceramics have been combined to surpass the individual disadvantages of each type of biomaterial and meet a broader range of requirements. Besides the composition of the scaffold, its fabrication is also crucial since it highly influences its architecture. Classical strategies as solvent casting and freeze-drying have been successfully used to develop porous scaffolds. Still, the control over the pore size and distribution, geometry, and interconnectivity has been shown to be a challenge. For so, additive manufacturing strategies, such as 3D printing, that enable the production, layer-by-layer, of more intricate and reproducible scaffolds have been pursued. Such strategies allow the recapitulation of environmental features of bone tissue with precision by printing different materials, growth factors, and cells, favoring the production of patient-specific scaffolds. Besides the study of scaffold-based strategies comprising osteoinductive scaffolds and osteogenic cells mimicking the intramembranous ossification process, scaffold-free strategies envision the simulation of the embryological process endochondral ossification has also been studied. Even so, the use of high cellular density structures, as cell pellets, spheroids, or organoids, faces significant issues concerning scalability and vascularization. Once more, printing strategies have emerged as a powerful tool, this time for the development of scaffold-free structures. In this sense, by enabling the bioprint of cell aggregates in a controlled manner, they can work as building blocks to produce organ-like structures. Furthermore, bone tissue is highly vascularized, presenting an intricate network that allows for the distribution of nutrients and oxygen, and waste removal. The design of approaches based on cells or biomolecular cues to induce vascularization has struggled to control the arrangement of the newly formed vascular network. Strategies to induce vascularization are often observed, but no evident control over the vascular network has been observed. For so, fabrication techniques and co-culture techniques have been pursued to obtain vessel-like structures within engineered pre-vascularized scaffolds, and cellular spheroids have been widely investigated to develop pre-vascularized cellular aggregates. Despite the advances achieved using such pre-vascularized systems, new advanced strategies have been studied to obtain larger structures and overcome the limitations regarding diffusion.

Combining different materials, processing techniques, and cells will be crucial to accomplish more successful bone tissue engineering approaches in the near future. Not only to mimic the transition within the bone and surrounding tissues, such as cartilage, tendons, or connective tissues, since such change typically exhibits different architectures, mechanical properties, and types of cells. But also to promote the interplay between cells and surrounding materials. An adaptive material capable of reacting upon cellular variations would enable native cell behavior, from cell spreading to cell migration and differentiation. Moreover, materials that adapt their form upon external stimuli, such as the ones studied for 4D printing, would enable the implantation into any site, even uneven defects, resulting in a higher probability of success. In fact, the 4D printing technique will offer unprecedented opportunities to produce complex environments that can be implanted into any defect.

As a final remark, regardless of the significant advances achieved in the bone tissue engineering field, especially in the development of scaffolds- and scaffold-free approaches, there are still some challenges to be overcome to boost their translation into the clinics.

Acknowledgments

F.R. Maia acknowledges the funds provided by the Research and Innovation Staff Exchanges (RISE) action (H2020 Marie Skłodowska-Curie actions) for funds obtained through the BAMOS project (H2020-MSCA-RISE-2016-73415), the R&D Project KOAT PTDC/BTMMAT/29760/2017 (POCI-01-0145-FEDER-029760), financed by the Portuguese Foundation for Science and Technology (FCT) and co-financed by FEDER and POCI, and FCT for her work contract under the Transitional Rule DL 57/2016 (CTTI-57/18-I3BS5). A. R. Bastos thanks the funds provided by FCT under the doctoral program in Tissue Engineering, Regenerative Medicine and Stem Cells (PD/BD/143043/2018).

References

[1] E.H. Schemitsch, Size matters: defining critical in bone defect Size!, J. Orthop. Trauma 31 (2017) S20–S22.
[2] W. Wang, K.W.K. Yeung, Bone grafts and biomaterials substitutes for bone defect repair: a review, Bioact. Mater. 2 (4) (2017) 224–247.
[3] D.W. Walmsley, J.P. Waddell, E.H. Schemitsch, Isolated head and liner exchange in revision hip arthroplasty 25 (4) (2017) 288–296.
[4] H. Qu, H. Fu, Z. Han, Y. Sun, Biomaterials for bone tissue engineering scaffolds: a review, RSC Adv. 9 (45) (2019) 26252–26262.
[5] D. Lopes, C. Martins-Cruz, M.B. Oliveira, J.F. Mano, Bone physiology as inspiration for tissue regenerative therapies, Biomaterials 185 (2018) 240–275.
[6] A.K. Nair, A. Gautieri, S.-W. Chang, M.J. Buehler, Molecular mechanics of mineralized collagen fibrils in bone, Nat. Commun. 4 (1) (2013) 1724.
[7] Z. Sheikh, S. Najeeb, Z. Khurshid, V. Verma, H. Rashid, M. Glogauer, Biodegradable materials for bone repair and tissue engineering applications, Materials 8 (9) (2015).
[8] A. Dhawan, P.M. Kennedy, E.B. Rizk, I.T. Ozbolat, Three-dimensional bioprinting for bone and cartilage restoration in orthopaedic surgery 27 (5) (2019) e215–e226.
[9] D. Zamani, F. Moztarzadeh, D. Bizari, Alginate-bioactive glass containing Zn and Mg composite scaffolds for bone tissue engineering, Int. J. Biol. Macromol. 137 (2019) 1256–1267.
[10] E. Salamanca, C.C. Hsu, H.M. Huang, N.C. Teng, C.T. Lin, Y.H. Pan, et al., Bone regeneration using a porcine bone substitute collagen composite in vitro and in vivo, Sci. Rep. 8 (1) (2018) 984.
[11] E. Stengelin, A. Kuzmina, G.L. Beltramo, M.F. Koziol, L. Besch, R. Schröder, et al., Bone scaffolds based on degradable vaterite/PEG-composite microgels, Adv. Healthc. Mater. 9 (11) (2020) 1901820.
[12] A. Esmaeilkhanian, F. Sharifianjazi, A. Abouchenari, A. Rouhani, N. Parvin, M. Irani, Synthesis and characterization of natural nano-hydroxyapatite derived from Turkey femur-bone waste, Appl. Biochem. Biotechnol. 189 (3) (2019) 919–932.
[13] M. Godoy-Gallardo, N. Portolés-Gil, A.M. López-Periago, C. Domingo, L. Hosta-Rigau, Multi-layered polydopamine coatings for the immobilization of growth factors onto highly-interconnected and bimodal PCL/HA-based scaffolds, Mater. Sci. Eng. C 117 (2020), 111245.
[14] S.-J. Wang, D. Jiang, Z.-Z. Zhang, Y.-R. Chen, Z.-D. Yang, J.-Y. Zhang, et al., Biomimetic nanosilica-collagen scaffolds for in situ bone regeneration: toward a cell-free, one-step surgery, Adv. Mater. 31 (49) (2019) 1904341.
[15] J. Zhang, E. Wehrle, P. Adamek, G.R. Paul, X.H. Qin, M. Rubert, et al., Optimization of mechanical stiffness and cell density of 3D bioprinted cell-laden scaffolds improves extracellular matrix mineralization and cellular organization for bone tissue engineering, Acta Biomater. 114 (2020) 307–322.
[16] T. Albrektsson, C. Johansson, Osteoinduction, osteoconduction and osseointegration, Eur. Spine J. 10 (2) (2001) S96–S101.
[17] F.R. Maia, S.J. Bidarra, P.L. Granja, C.C. Barrias, Functionalization of biomaterials with small osteoinductive moieties, Acta Biomater. 9 (11) (2013) 8773–8789.

[18] F.R. Maia, K.B. Fonseca, G. Rodrigues, P.L. Granja, C.C. Barrias, Matrix-driven formation of mesenchymal stem cell-extracellular matrix microtissues on soft alginate hydrogels, Acta Biomater. 10 (7) (2014) 3197–3208.

[19] A. Ho-Shui-Ling, J. Bolander, L.E. Rustom, A.W. Johnson, F.P. Luyten, C. Picart, Bone regeneration strategies: engineered scaffolds, bioactive molecules and stem cells current stage and future perspectives, Biomaterials 180 (2018) 143–162.

[20] G.G. Walmsley, R.C. Ransom, E.R. Zielins, T. Leavitt, J.S. Flacco, M.S. Hu, et al., Stem cells in bone regeneration, Stem Cell Rev. Rep. 12 (5) (2016) 524–529.

[21] A.O. Luby, K. Ranganathan, J.V. Lynn, N.S. Nelson, A. Donneys, S.R. Buchman, Stem cells for bone regeneration: current state and future directions, J. Craniofac. Surg. 30 (3) (2019).

[22] P.A. Zuk, M. Zhu, P. Ashjian, D.A. De Ugarte, J.I. Huang, H. Mizuno, et al., Human adipose tissue is a source of multipotent stem cells, Mol. Biol. Cell 13 (12) (2002) 4279–4295.

[23] H. Elkhenany, L. Amelse, M. Caldwell, R. Abdelwahed, M. Dhar, Impact of the source and serial passaging of goat mesenchymal stem cells on osteogenic differentiation potential: implications for bone tissue engineering, J. Anim. Sci. Biotechnol. 7 (2016) 16.

[24] H. Lin, Y. Tang, T.P. Lozito, N. Oyster, B. Wang, R.S. Tuan, Efficient in vivo bone formation by BMP-2 engineered human mesenchymal stem cells encapsulated in a projection stereolithographically fabricated hydrogel scaffold, Stem. Cell Res. Ther. 10 (1) (2019) 254.

[25] C.J. Kowalczewski, J.M. Saul, Biomaterials for the delivery of growth factors and other therapeutic agents in tissue engineering approaches to bone regeneration, Front. Pharmacol. 9 (513) (2018).

[26] A. Marrella, T.Y. Lee, D.H. Lee, S. Karuthedom, D. Syla, A. Chawla, et al., Engineering vascularized and innervated bone biomaterials for improved skeletal tissue regeneration, Mater. Today 21 (4) (2018) 362–376.

[27] R. Burdis, D.J. Kelly, Biofabrication and bioprinting using cellular aggregates, microtissues and organoids for the engineering of musculoskeletal tissues, Acta Biomater. 126 (2021) 1–14, https://doi.org/10.1016/j.actbio.2021.03.016.

[28] G.D. DuRaine, W.E. Brown, J.C. Hu, K.A. Athanasiou, Emergence of scaffold-free approaches for tissue engineering musculoskeletal cartilages, Ann. Biomed. Eng. 43 (3) (2015) 543–554.

[29] T. Ghassemi, A. Shahroodi, M.H. Ebrahimzadeh, A. Mousavian, J. Movaffagh, A. Moradi, Current concepts in scaffolding for bone tissue engineering, Arch. Bone Joint Surg. 6 (2) (2018) 90–99.

[30] T. Tariverdian, F. Sefat, M. Gelinsky, M. Mozafari, Scaffold for bone tissue engineering, in: M. Mozafari, F. Sefat, A. Atala (Eds.), Handbook of Tissue Engineering Scaffolds: Volume One, 10, Woodhead Publishing, 2019, pp. 189–209.

[31] T. Marew, G. Birhanu, Three dimensional printed nanostructure biomaterials for bone tissue engineering, Regen. Ther. 18 (2021) 102–111.

[32] W. Xue, B.V. Krishna, A. Bandyopadhyay, S. Bose, Processing and biocompatibility evaluation of laser processed porous titanium, Acta Biomater. 3 (6) (2007) 1007–1018.

[33] Y. Kuboki, Q. Jin, M. Kikuchi, J. Mamood, H. Takita, Geometry of artificial ECM: sizes of pores controlling phenotype expression in BMP-induced osteogenesis and chondrogenesis, Connect. Tissue Res. 43 (2–3) (2002) 529–534.

[34] M.-q. Cheng, T. Wahafu, G.-f. Jiang, W. Liu, Y.-q. Qiao, X.-c. Peng, et al., A novel open-porous magnesium scaffold with controllable microstructures and properties for bone regeneration, Sci. Rep. 6 (1) (2016) 24134.

[35] C.M. Murphy, M.G. Haugh, F.J. O'Brien, The effect of mean pore size on cell attachment, proliferation and migration in collagen–glycosaminoglycan scaffolds for bone tissue engineering, Biomaterials 31 (3) (2010) 461–466.

[36] S. Bose, S. Vahabzadeh, A. Bandyopadhyay, Bone tissue engineering using 3D printing, Mater. Today 16 (12) (2013) 496–504.

[37] K. Stuckensen, A. Schwab, M. Knauer, E. Muiños-López, F. Ehlicke, J. Reboredo, et al., Tissue mimicry in morphology and composition promotes hierarchical matrix remodeling of invading stem cells in osteochondral and meniscus scaffolds, Adv. Mater. 30 (28) (2018) 1706754.

[38] F. Donnaloja, E. Jacchetti, M. Soncini, M.T. Raimondi, Natural and synthetic polymers for bone scaffolds optimization, Polymers (Basel) 12 (4) (2020) 905.

[39] E. Kon, G. Filardo, F. Perdisa, G. Venieri, M. Marcacci, Clinical results of multilayered biomaterials for osteochondral regeneration, J. Exp. Orthop. 1 (1) (2014) 10.

[40] G.A. Rico-Llanos, S. Borrego-González, M. Moncayo-Donoso, J. Becerra, R. Visser, Collagen type I biomaterials as scaffolds for bone tissue engineering, Polymers (Basel) 13 (4) (2021) 599.

[41] K. Adamiak, A. Sionkowska, Current methods of collagen cross-linking: review, Int. J. Biol. Macromol. 161 (2020) 550–560.

[42] Z. Jing, Y. Wu, W. Su, M. Tian, W. Jiang, L. Cao, et al., Carbon nanotube reinforced collagen/hydroxyapatite scaffolds improve bone tissue formation in vitro and in vivo, Ann. Biomed. Eng. 45 (9) (2017) 2075–2087.

[43] F.R. Maia, M. Barbosa, D.B. Gomes, N. Vale, P. Gomes, P.L. Granja, et al., Hydrogel depots for local co-delivery of osteoinductive peptides and mesenchymal stem cells, J. Control. Release 189 (2014) 158–168.

[44] A.C. Hernández-González, L. Téllez-Jurado, L.M. Rodríguez-Lorenzo, Alginate hydrogels for bone tissue engineering, from injectables to bioprinting: a review, Carbohydr. Polym. 229 (2020), 115514.

[45] R. Ahmad Raus, W.M.F. Wan Nawawi, R.R. Nasaruddin, Alginate and alginate composites for biomedical applications, Asian J. Pharm. Sci. 16 (2020) 280–306, https://doi.org/10.1016/j.ajps.2020.10.001.

[46] M.F. Raquel, Ana H. Lourenço, Pedro L. Granja, Raquel M. Gonçalves, Cristina C. Barrias, Effect of cell density on mesenchymal stem cells aggregation in RGD-alginate 3D matrices under osteoinductive conditions 14 (6) (2014) 759–771.

[47] K.B. Fonseca, F.R. Maia, F.A. Cruz, D. Andrade, M.A. Juliano, P.L. Granja, et al., Enzymatic, physicochemical and biological properties of MMP-sensitive alginate hydrogels, Soft Matter 9 (12) (2013) 3283–3292.

[48] C. Xu, J. Xu, L. Xiao, Z. Li, Y. Xiao, M. Dargusch, et al., Double-layered microsphere based dual growth factor delivery system for guided bone regeneration, RSC Adv. 8 (30) (2018) 16503–16512.

[49] P. Bhattacharjee, B. Kundu, D. Naskar, H.W. Kim, T.K. Maiti, D. Bhattacharya, et al., Silk scaffolds in bone tissue engineering: an overview, Acta Biomater. 63 (2017) 1–17.

[50] W. Zaoming, R. Codina, E. Fernández-Caldas, R.F. Lockey, Partial characterization of the silk allergens in mulberry silk extract, J Investig Allergol Clin Immunol 6 (4) (1996) 237–241.

[51] J. Melke, S. Midha, S. Ghosh, K. Ito, S. Hofmann, Silk fibroin as biomaterial for bone tissue engineering, Acta Biomater. 31 (2016) 1–16.

[52] L.-D. Koh, Y. Cheng, C.-P. Teng, Y.-W. Khin, X.-J. Loh, S.-Y. Tee, et al., Structures, mechanical properties and applications of silk fibroin materials, Prog. Polym. Sci. 46 (2015) 86–110.

[53] J.H. Choi, D.K. Kim, J.E. Song, J.M. Oliveira, R.L. Reis, G. Khang, Silk fibroin-based scaffold for bone tissue engineering, Adv. Exp. Med. Biol. 1077 (2018) 371–387.

[54] C. Holland, K. Numata, J. Rnjak-Kovacina, F.P. Seib, The biomedical use of silk: past, present, future, Adv. Healthc. Mater. 8 (1) (2019) 1800465.

[55] H. Zhang, R. You, K. Yan, Z. Lu, Q. Fan, X. Li, et al., Silk as templates for hydroxyapatite biomineralization: a comparative study of Bombyx mori and Antheraea pernyi silkworm silks, Int. J. Biol. Macromol. 164 (2020) 2842–2850.

[56] B. Kundu, V. Brancato, J.M. Oliveira, V.M. Correlo, R.L. Reis, S.C. Kundu, Silk fibroin promotes mineralization of gellan gum hydrogels, Int. J. Biol. Macromol. 153 (2020) 1328–1334.

[57] R. LogithKumar, A. KeshavNarayan, S. Dhivya, A. Chawla, S. Saravanan, N. Selvamurugan, A review of chitosan and its derivatives in bone tissue engineering, Carbohydr. Polym. 151 (2016) 172–188.

[58] J. Jiao, J. Huang, Z. Zhang, Hydrogels based on chitosan in tissue regeneration: how do they work? A mini review, J. Appl. Polym. Sci. 136 (13) (2019) 47235.

[59] K. Lavanya, S.V. Chandran, K. Balagangadharan, N. Selvamurugan, Temperature- and pH-responsive chitosan-based injectable hydrogels for bone tissue engineering, Mater. Sci. Eng. C Mater. Biol. Appl. 111 (2020), 110862.

[60] E.I. Akpan, O.P. Gbenebor, S.O. Adeosun, O. Cletus, Chapter 16 - Chitin and chitosan composites for bone tissue regeneration, in: S. Gopi, S. Thomas, A. Pius (Eds.), Handbook of Chitin and Chitosan, Elsevier, 2020, pp. 499–553.

[61] K. Zafeiris, D. Brasinika, A. Karatza, E. Koumoulos, I.K. Karoussis, K. Kyriakidou, et al., Additive manufacturing of hydroxyapatite–chitosan–genipin composite scaffolds for bone tissue engineering applications, Mater. Sci. Eng. C 119 (2021), 111639.

[62] G. Chen, Y. Lv, Decellularized bone matrix scaffold for bone regeneration, Methods Mol. Biol. (Clifton, NJ) 1577 (2018) 239–254.

[63] Y.S. Kim, M. Majid, A.J. Melchiorri, A.G. Mikos, Applications of decellularized extracellular matrix in bone and cartilage tissue engineering, Bioeng. Transl. Med. 4 (1) (2018) 83–95.

[64] G. Chen, Y. Lv, Decellularized bone matrix scaffold for bone regeneration, in: K. Turksen (Ed.), Decellularized Scaffolds and Organogenesis: Methods and Protocols, Springer New York, New York, NY, 2018, pp. 239–254.

[65] D.A. Taylor, L.C. Sampaio, Z. Ferdous, A.S. Gobin, L.J. Taite, Decellularized matrices in regenerative medicine, Acta Biomater. 74 (2018) 74–89.

[66] B.T. Wilks, E.B. Evans, M.N. Nakhla, J.R. Morgan, Directing fibroblast self-assembly to fabricate highly-aligned, collagen-rich matrices, Acta Biomater. 81 (2018) 70–79.

[67] M. Assunção, D. Dehghan-Baniani, C.H.K. Yiu, T. Später, S. Beyer, A. Blocki, Cell-derived extracellular matrix for tissue engineering and regenerative medicine, Front. Bioeng. Biotechnol. 8 (1378) (2020).

[68] E.P. McNeill, S. Zeitouni, S. Pan, A. Haskell, M. Cesarek, D. Tahan, et al., Characterization of a pluripotent stem cell-derived matrix with powerful osteoregenerative capabilities, Nat. Commun. 11 (1) (2020) 3025.

[69] F.R. Maia, R.L. Reis, Oliveira J.M. Chapter, 3 - Decellularized hASCs-derived matrices as biomaterials for 3D in vitro approaches, in: D. Caballero, S.C. Kundu, R.L. Reis (Eds.), Methods in Cell Biology, Academic Press, 2020, pp. 45–58.

[70] M.S. Carvalho, J.C. Silva, R.N. Udangawa, J.M.S. Cabral, F.C. Ferreira, C.L. da Silva, et al., Co-culture cell-derived extracellular matrix loaded electrospun microfibrous scaffolds for bone tissue engineering, Mater. Sci. Eng. C 99 (2019) 479–490.

[71] A. Escudero-Castellanos, B.E. Ocampo-García, M.V. Domínguez-García, J. Flores-Estrada, M.V. Flores-Merino, Hydrogels based on poly(ethylene glycol) as scaffolds for tissue engineering application: biocompatibility assessment and effect of the sterilization process, J. Mater. Sci. Mater. Med. 27 (12) (2016) 176.

[72] L. Ouyang, Y. Dan, Z. Shao, S. Yang, C. Yang, G. Liu, et al., MMP-sensitive PEG hydrogel modified with RGD promotes bFGF, VEGF and EPC-mediated angiogenesis, Exp. Ther. Med. 18 (4) (2019) 2933–2941.

[73] S. Sreekumaran, A. Radhakrishnan, A.A. Rauf, G.M. Kurup, Nanohydroxyapatite incorporated photocrosslinked gelatin methacryloyl/poly(ethylene glycol) diacrylate hydrogel for bone tissue engineering, Prog Biomater. 10 (1) (2021) 43–51.

[74] A.S. Chahal, M. Schweikle, A.-M. Lian, J.E. Reseland, H.J. Haugen, H. Tiainen, Osteogenic potential of poly(ethylene glycol)-amorphous calcium phosphate composites on human mesenchymal stem cells, J. Tissue Eng. 11 (2020), 2041731420926840.

[75] P. Gentile, V. Chiono, I. Carmagnola, P.V. Hatton, An overview of Poly(lactic-co-glycolic) acid (PLGA)-based biomaterials for bone tissue engineering, Int. J. Mol. Sci. 15 (3) (2014) 3640–3659.

[76] X. Liang, P. Duan, J. Gao, R. Guo, Z. Qu, X. Li, et al., Bilayered PLGA/PLGA-HAp composite scaffold for osteochondral tissue engineering and tissue regeneration, ACS Biomater. Sci. Eng. 4 (10) (2018) 3506–3521.

[77] A.J.R. Lasprilla, G.A.R. Martinez, B.H. Lunelli, A.L. Jardini, R.M. Filho, Poly-lactic acid synthesis for application in biomedical devices — a review, Biotechnol. Adv. 30 (1) (2012) 321–328.

[78] G. Narayanan, V.N. Vernekar, E.L. Kuyinu, C.T. Laurencin, Poly (lactic acid)-based biomaterials for orthopaedic regenerative engineering, Adv. Drug Deliv. Rev. 107 (2016) 247–276.

[79] M. Santoro, S.R. Shah, J.L. Walker, A.G. Mikos, Poly(lactic acid) nanofibrous scaffolds for tissue engineering, Adv. Drug Deliv. Rev. 107 (2016) 206–212.

[80] F.C. Oliveira, J.O. Carvalho, L.S.S.M. Magalhães, J.M. da Silva, S.R. Pereira, A. L. Gomes Júnior, et al., Biomineralization inspired engineering of nanobiomaterials promoting bone repair, Mater. Sci. Eng. C 120 (2021), 111776.

[81] R. Dwivedi, S. Kumar, R. Pandey, A. Mahajan, D. Nandana, D.S. Katti, et al., Polycaprolactone as biomaterial for bone scaffolds: review of literature, J. Oral Biol. Craniofac. Res. 10 (1) (2020) 381–388.

[82] E. Stastna, K. Castkova, J. Rahel, Influence of hydroxyapatite nanoparticles and surface plasma treatment on bioactivity of polycaprolactone nanofibers, Polymers (Basel) 12 (9) (2020) 1877.

[83] S. Pina, V.P. Ribeiro, C.F. Marques, F.R. Maia, T.H. Silva, R.L. Reis, et al., Scaffolding strategies for tissue engineering and regenerative medicine applications, Materials 12 (11) (2019) 1824.

[84] M.-P. Ginebra, M. Espanol, Y. Maazouz, V. Bergez, D. Pastorino, Bioceramics and bone healing, EFORT Open Rev. 3 (5) (2018) 173–183.

[85] S. Pina, R.F. Canadas, G. Jiménez, M. Perán, J.A. Marchal, R.L. Reis, et al., Biofunctional ionic-doped calcium phosphates: silk fibroin composites for bone tissue engineering scaffolding, Cells Tissues Organs 204 (3–4) (2017) 150–163.

[86] S. Samavedi, A.R. Whittington, A.S. Goldstein, Calcium phosphate ceramics in bone tissue engineering: a review of properties and their influence on cell behavior, Acta Biomater. 9 (9) (2013) 8037–8045.

[87] J.M. Bouler, P. Pilet, O. Gauthier, E. Verron, Biphasic calcium phosphate ceramics for bone reconstruction: a review of biological response, Acta Biomater. 53 (2017) 1–12.

[88] R. Trombetta, J.A. Inzana, E.M. Schwarz, S.L. Kates, H.A. Awad, 3D printing of calcium phosphate ceramics for bone tissue engineering and drug delivery, Ann. Biomed. Eng. 45 (1) (2017) 23–44.

[89] P. Dee, H.Y. You, S.-H. Teoh, H. Le Ferrand, Bioinspired approaches to toughen calcium phosphate-based ceramics for bone repair, J. Mech. Behav. Biomed. Mater. 112 (2020), 104078.

[90] J. Tuukkanen, M. Nakamura, Hydroxyapatite as a nanomaterial for advanced tissue engineering and drug therapy, Curr. Pharm. Des. 23 (26) (2017) 3786–3793.

[91] J. Jeong, J.H. Kim, J.H. Shim, N.S. Hwang, C.Y. Heo, Bioactive calcium phosphate materials and applications in bone regeneration, Biomater. Res. 23 (1) (2019) 4.

[92] J.H. Kim, D.K. Kim, O.J. Lee, H.W. Ju, J.M. Lee, B.M. Moon, et al., Osteoinductive silk fibroin/titanium dioxide/hydroxyapatite hybrid scaffold for bone tissue engineering, Int. J. Biol. Macromol. 82 (2016) 160–167.

[93] M.G. Manda, L.P. da Silva, M.T. Cerqueira, D.R. Pereira, M.B. Oliveira, J.F. Mano, et al., Gellan gum-hydroxyapatite composite spongy-like hydrogels for bone tissue engineering, J. Biomed. Mater. Res. A 106 (2) (2018) 479–490.

[94] F.R. Maia, D.S. Musson, D. Naot, L.P. da Silva, A.R. Bastos, J.B. Costa, et al., Differentiation of osteoclast precursors on gellan gum-based spongy-like hydrogels for bone tissue engineering, Biom. Mater. (Bristol, England) 13 (3) (2018), 035012.

[95] R.G. Carrodeguas, S. De Aza, α-tricalcium phosphate: synthesis, properties and biomedical applications, Acta Biomater. 7 (10) (2011) 3536–3546.

[96] S.K. Nandi, G. Fielding, D. Banerjee, A. Bandyopadhyay, S. Bose, 3D printed β-TCP bone tissue engineering scaffolds: effects of chemistry on in vivo biological properties in a rabbit tibia model, J. Mater. Res. 33 (14) (2018) 1939–1947.

[97] 97. H. Tebyanian, M.H. Norahan, H. Eyni, M. Movahedin, S.J. Mortazavi, A. Karami, et al., J. Appl. Biomater. Funct. Mater. 17 (1) (2019);
97. H. Tebyanian, M.H. Norahan, H. Eyni, M. Movahedin, S.J. Mortazavi, A. Karami, et al., J. Appl. Biomater. Funct. Mater. 17 (1) (2019).

[98] S.E. Kim, K. Park, Recent advances of biphasic calcium phosphate bioceramics for bone tissue regeneration, Adv. Exp. Med. Biol. 1250 (2020) 177–188.

[99] M. Rezaei, M. Farhadian, A.M. Rashidi, M. Saeidipour, M. Manshaei, M. Rezaee, Nano-biphasic calcium phosphate ceramic for the repair of bone defects, J. Craniofac. Surg. 29 (6) (2018) e543–e548.

[100] S. Heng, Z. Lu, Q. Liu, T. Jiang, M. He, F. Song, et al., Injectable calcium phosphate ceramics prevent osteoclastic differentiation and osteoporotic bone loss: potential applications for regional osteolysis, Mater. Sci. Eng. C 110 (2020), 110691.

[101] G. Turnbull, J. Clarke, F. Picard, P. Riches, L. Jia, F. Han, et al., 3D bioactive composite scaffolds for bone tissue engineering, Bioact. Mater. 3 (3) (2017) 278–314.

[102] G.S. Diogo, C.F. Marques, C.G. Sotelo, R.I. Pérez-Martín, R.P. Pirraco, R.L. Reis, et al., Cell-laden biomimetically mineralized shark-skin-collagen-based 3D printed hydrogels for the engineering of hard tissues, ACS Biomater. Sci. Eng. 6 (6) (2020) 3664–3672.

[103] D. Lee, M. Wufuer, I. Kim, T.H. Choi, B.J. Kim, H.G. Jung, et al., Sequential dual-drug delivery of BMP-2 and alendronate from hydroxyapatite-collagen scaffolds for enhanced bone regeneration, Sci. Rep. 11 (1) (2021) 746.

[104] K. Szurkowska, P. Kazimierczak, J. Kolmas, Mg, Si—Co-substituted hydroxyapatite/alginate composite beads loaded with raloxifene for potential use in bone tissue regeneration, Int. J. Mol. Sci. 22 (6) (2021) 2933.

[105] C. Zheng, S. Attarilar, K. Li, C. Wang, J. Liu, L. Wang, et al., 3D-printed HA15-loaded β-tricalcium phosphate/poly (lactic-co-glycolic acid) bone tissue scaffold promotes bone regeneration in rabbit radial defects, Int J Bioprint. 7 (2021) 317-317, https://doi.org/10.18063/ijb.v7i1.317.

[106] A.G. Krishnan, R. Biswas, D. Menon, M.B. Nair, Biodegradable nanocomposite fibrous scaffold mediated local delivery of vancomycin for the treatment of MRSA infected experimental osteomyelitis, Biomater. Sci. 8 (9) (2020) 2653–2665.

[107] V. Guarino, S. Scaglione, M. Sandri, S. Sprio, A. Tampieri, L. Ambrosio, Chapter 10 - composite scaffolds for bone and osteochondral defects, in: A.-M. Holban, A. M. Grumezescu (Eds.), Materials for Biomedical Engineering, Elsevier, 2019, pp. 297–337.

[108] D. Xu, G. Cheng, J. Dai, Z. Li, Bi-layered composite scaffold for repair of the osteochondral defects, Adv. Wound Care 10 (2020) 401–414, https://doi.org/10.1089/wound.2019.1140.

[109] F.D. Cojocaru, V. Balan, I.M. Popa, A. Munteanu, A. Anghelache, L. Verestiuc, Magnetic composite scaffolds for potential applications in radiochemotherapy of malignant bone tumors, Medicina (Kaunas) 55 (5) (2019) 153.

[110] S. Pina, V.P. Ribeiro, C.F. Marques, F.R. Maia, T.H. Silva, R.L. Reis, et al., Scaffolding strategies for tissue engineering and regenerative medicine applications, Materials (Basel, Switzerland) 12 (11) (2019) 1824.

[111] C. Wang, W. Huang, Y. Zhou, L. He, Z. He, Z. Chen, et al., 3D printing of bone tissue engineering scaffolds, Bioact. Mater. 5 (1) (2020) 82–91.

[112] M. Salah, L. Tayebi, K. Moharamzadeh, F.B. Naini, Three-dimensional bio-printing and bone tissue engineering: technical innovations and potential applications in maxillofacial reconstructive surgery, Maxillofac Plast Reconstr Surg. 42 (1) (2020) 18.

[113] J.B. Costa, J. Park, A.M. Jorgensen, J. Silva-Correia, R.L. Reis, J.M. Oliveira, et al., 3D bioprinted highly elastic hybrid constructs for advanced fibrocartilaginous tissue regeneration, Chem. Mater. 32 (19) (2020) 8733–8746.

[114] J.B. Costa, J. Silva-Correia, V.P. Ribeiro, Morais A. da Silva, J.M. Oliveira, R. L. Reis, Engineering patient-specific bioprinted constructs for treatment of degenerated intervertebral disc, Mater. Today Commun. 19 (2019) 506–512.

[115] J.B. Costa, J. Silva-Correia, S. Pina, Morais A. da Silva, S. Vieira, H. Pereira, et al., Indirect printing of hierarchical patient-specific scaffolds for meniscus tissue engineering, Bio-Des. Manuf. 2 (4) (2019) 225–241.

[116] M. Vaezi, G. Zhong, H. Kalami, S. Yang, 10 - extrusion-based 3D printing technologies for 3D scaffold engineering, in: Y. Deng, J. Kuiper (Eds.), Functional 3D Tissue Engineering Scaffolds, Woodhead Publishing, 2018, pp. 235–254.

[117] G. Gao, B.S. Kim, J. Jang, D.-W. Cho, Recent strategies in extrusion-based three-dimensional cell printing toward organ biofabrication, ACS Biomater. Sci. Eng. 5 (3) (2019) 1150–1169.

[118] L. Diaz-Gomez, M.E. Elizondo, P.D. Kontoyiannis, G.L. Koons, B. Dacunha-Marinho, X. Zhang, et al., Three-dimensional extrusion printing of porous scaffolds using storable ceramic inks, Tissue Eng Part C Methods 26 (6) (2020) 292–305.

[119] X. Ma, J. Liu, W. Zhu, M. Tang, N. Lawrence, C. Yu, et al., 3D bioprinting of functional tissue models for personalized drug screening and in vitro disease modeling, Adv. Drug Deliv. Rev. 132 (2018) 235–251.

[120] B. Byambaa, N. Annabi, K. Yue, G. Trujillo-de Santiago, M.M. Alvarez, W. Jia, et al., Bioprinted osteogenic and vasculogenic patterns for engineering 3D bone tissue, Adv. Healthc. Mater. 6 (16) (2017) 1700015.

[121] Ž.P. Kačarević, P.M. Rider, S. Alkildani, S. Retnasingh, R. Smeets, O. Jung, et al., An introduction to 3D bioprinting: possibilities, challenges and future aspects, Materials 11 (11) (2018) 2199.

[122] T. Xu, W. Zhao, J.-M. Zhu, M.Z. Albanna, J.J. Yoo, A. Atala, Complex heterogeneous tissue constructs containing multiple cell types prepared by inkjet printing technology, Biomaterials 34 (1) (2013) 130–139.

[123] Y. Guo, H.S. Patanwala, B. Bognet, A.W.K. Ma, Inkjet and inkjet-based 3D printing: connecting fluid properties and printing performance, Rapid Prototyp. J. 23 (3) (2017) 562–576.

[124] A.K. Miri, I. Mirzaee, S. Hassan, S. Mesbah Oskui, D. Nieto, A. Khademhosseini, et al., Effective bioprinting resolution in tissue model fabrication, Lab Chip 19 (11) (2019) 2019–2037.

[125] J. Li, F. Rossignol, J. Macdonald, Inkjet printing for biosensor fabrication: combining chemistry and technology for advanced manufacturing, Lab Chip 15 (12) (2015) 2538–2558.

[126] Z. Zhou, L. Ruiz Cantu, X. Chen, M.R. Alexander, C.J. Roberts, R. Hague, et al., High-throughput characterization of fluid properties to predict droplet ejection for three-dimensional inkjet printing formulations, Addit. Manuf. 29 (2019), 100792.

[127] G. Gao, T. Yonezawa, K. Hubbell, G. Dai, X. Cui, Inkjet-bioprinted acrylated peptides and PEG hydrogel with human mesenchymal stem cells promote robust bone and cartilage formation with minimal printhead clogging, Biotechnol. J. 10 (10) (2015) 1568–1577.

[128] T. Genova, I. Roato, M. Carossa, C. Motta, D. Cavagnetto, F. Mussano, Advances on bone substitutes through 3D bioprinting, Int. J. Mol. Sci. 21 (19) (2020) 7012.

[129] G. Gao, A.F. Schilling, K. Hubbell, T. Yonezawa, D. Truong, Y. Hong, et al., Improved properties of bone and cartilage tissue from 3D inkjet-bioprinted human mesenchymal stem cells by simultaneous deposition and photocrosslinking in PEG-GelMA, Biotechnol. Lett. 37 (11) (2015) 2349–2355.

[130] J.P. Vanderburgh, S.J. Fernando, A.R. Merkel, J.A. Sterling, S.A. Guelcher, Fabrication of trabecular bone-templated tissue-engineered constructs by 3D inkjet printing, Adv. Healthc. Mater. 6 (22) (2017) 1700369.

[131] I. Matai, G. Kaur, A. Seyedsalehi, A. McClinton, C.T. Laurencin, Progress in 3D bioprinting technology for tissue/organ regenerative engineering, Biomaterials 226 (2020), 119536.

[132] Z. Hadisi, T. Walsh, S.M.H. Dabiri, A. Seyfoori, B. Godeau, G. Charest, et al., 3D printing for the future of medicine, J. 3D Print. Med. 4 (1) (2020) 45–67.

[133] F. Guillemot, A. Souquet, S. Catros, B. Guillotin, Laser-assisted cell printing: principle, physical parameters versus cell fate and perspectives in tissue engineering, Nanomedicine 5 (3) (2010) 507–515.

[134] S. Derakhshanfar, R. Mbeleck, K. Xu, X. Zhang, W. Zhong, M. Xing, 3D bioprinting for biomedical devices and tissue engineering: a review of recent trends and advances, Bioact. Mater. 3 (2) (2018) 144–156.

[135] V. Keriquel, H. Oliveira, M. Rémy, S. Ziane, S. Delmond, B. Rousseau, et al., In situ printing of mesenchymal stromal cells, by laser-assisted bioprinting, for in vivo bone regeneration applications, Sci. Rep. 7 (1) (2017) 1778.

[136] F. Kawecki, W.P. Clafshenkel, F.A. Auger, J.M. Bourget, J. Fradette, R. Devillard, Self-assembled human osseous cell sheets as living biopapers for the laser-assisted bioprinting of human endothelial cells, Biofabrication 10 (3) (2018), 035006.

[137] A.P. Moreno Madrid, S.M. Vrech, M.A. Sanchez, A.P. Rodriguez, Advances in additive manufacturing for bone tissue engineering scaffolds, Mater. Sci. Eng. C 100 (2019) 631–644.

[138] Y. Luo, H. Pan, J. Jiang, C. Zhao, J. Zhang, P. Chen, et al., Desktop-stereolithography 3D printing of a polyporous extracellular matrix bioink for bone defect regeneration, Front. Bioeng. Biotechnol. 8 (1300) (2020).

[139] H. Kumar, K. Kim, Stereolithography 3D bioprinting, Methods Mol. Biol. (Clifton, NJ) 2140 (2020) 93–108.

[140] F.P.W. Melchels, J. Feijen, D.W. Grijpma, A review on stereolithography and its applications in biomedical engineering, Biomaterials 31 (24) (2010) 6121–6130.

[141] N. Anandakrishnan, H. Ye, Z. Guo, Z. Chen, K.I. Mentkowski, J.K. Lang, et al., Fast stereolithography printing of large-scale biocompatible hydrogel models, Adv. Healthc. Mater. 10 (10) (2021) 2002103.

[142] Z. Wang, R. Abdulla, B. Parker, R. Samanipour, S. Ghosh, K. Kim, A simple and high-resolution stereolithography-based 3D bioprinting system using visible light crosslinkable bioinks, Biofabrication 7 (4) (2015), 045009.

[143] Z. Jiao, B. Luo, S. Xiang, H. Ma, Y. Yu, W. Yang, 3D printing of HA / PCL composite tissue engineering scaffolds 2 (4) (2019) 196–202.

[144] J. Babilotte, B. Martin, V. Guduric, R. Bareille, R. Agniel, S. Roques, et al., Development and characterization of a PLGA-HA composite material to fabricate 3D-printed scaffolds for bone tissue engineering, Mater. Sci. Eng. C 118 (2021), 111334.

[145] V. Melčová, K. Svoradová, P. Menčík, S. Kontárová, M. Rampichová, V. Hedvičáková, et al., FDM 3D printed composites for bone tissue engineering based on plasticized Poly(3-hydroxybutyrate)/poly(d, l-lactide), Blends Polym. (Basel) 12 (12) (2020).

[146] J.T. Schantz, T.C. Lim, C. Ning, S.H. Teoh, K.C. Tan, S.C. Wang, et al., Cranioplasty after trephination using a novel biodegradable burr hole cover: technical case report, Neurosurgery 58 (1 Suppl) (2006), ONS-E176 discussion ONS-E.

[147] J.C. Silva, M.S. Carvalho, R.N. Udangawa, C.S. Moura, J.M.S. Cabral, C. LdS, et al., Extracellular matrix decorated polycaprolactone scaffolds for improved mesenchymal stem/stromal cell osteogenesis towards a patient-tailored bone tissue engineering approach, J Biomed Mater Res B Appl Biomater 108 (5) (2020) 2153–2166.

[148] F. Fina, C.M. Madla, A. Goyanes, J. Zhang, S. Gaisford, A.W. Basit, Fabricating 3D printed orally disintegrating printlets using selective laser sintering, Int. J. Pharm. 541 (1–2) (2018) 101–107.

[149] W. Tan, C. Gao, P. Feng, Q. Liu, C. Liu, Z. Wang, et al., Dual-functional scaffolds of poly(L-lactic acid)/nanohydroxyapatite encapsulated with metformin: simultaneous enhancement of bone repair and bone tumor inhibition, Mater. Sci. Eng. C Mater. Biol. Appl. 120 (2021), 111592.

[150] Z. Meng, J. He, Z. Cai, M. Zhang, J. Zhang, R. Ling, et al., In-situ re-melting and re-solidification treatment of selective laser sintered polycaprolactone lattice scaffolds for improved filament quality and mechanical properties, Biofabrication 12 (3) (2020), 035012.

[151] Z. Wan, P. Zhang, Y. Liu, L. Lv, Y. Zhou, Four-dimensional bioprinting: current developments and applications in bone tissue engineering, Acta Biomater. 101 (2020) 26–42.

[152] C. Wang, H. Yue, J. Liu, Q. Zhao, Z. He, K. Li, et al., Advanced reconfigurable scaffolds fabricated by 4D printing for treating critical-size bone defects of irregular shapes, Biofabrication 12 (4) (2020), 045025.

[153] A. De Pieri, Y. Rochev, D.I. Zeugolis, Scaffold-free cell-based tissue engineering therapies: advances, shortfalls and forecast, npj Regenerative Medicine 6 (1) (2021) 18.

[154] M. Jakob, F. Saxer, C. Scotti, S. Schreiner, P. Studer, A. Scherberich, et al., Perspective on the evolution of cell-based bone tissue engineering strategies, Eur. Surg. Res. 49 (1) (2012) 1–7.

[155] R. Fu, C. Liu, Y. Yan, Q. Li, R.-L. Huang, Bone defect reconstruction via endochondral ossification: a developmental engineering strategy, J. Tissue Eng. 12 (2021), 20417314211004211.

[156] J.N. Fisher, G.M. Peretti, C. Scotti, Stem cells for bone regeneration: from cell-based therapies to decellularised engineered extracellular matrices, 2016, 2016: 9352598.

[157] D. Gawlitta, K.E. Benders, J. Visser, A.S. van der Sar, D.H. Kempen, L.F. Theyse, et al., Decellularized cartilage-derived matrix as substrate for endochondral bone regeneration, Tissue Eng. A 21 (3–4) (2015) 694–703.

[158] N. Harada, Y. Watanabe, K. Sato, S. Abe, K. Yamanaka, Y. Sakai, et al., Bone regeneration in a massive rat femur defect through endochondral ossification achieved with chondrogenically differentiated MSCs in a degradable scaffold, Biomaterials 35 (27) (2014) 7800–7810.

[159] S. Pigeot, P.E. Bourgine, J. Claude, C. Scotti, A. Papadimitropoulos, A. Todorov, et al., Orthotopic bone formation by streamlined engineering and devitalization of human hypertrophic cartilage, Int. J. Mol. Sci. 21 (19) (2020) 7233.

[160] M. Zhang, J. Shi, M. Xie, J. Wen, K. Niibe, X. Zhang, et al., Recapitulation of cartilage/bone formation using iPSCs via biomimetic 3D rotary culture approach for developmental engineering, Biomaterials 260 (2020), 120334.

[161] C. Scotti, B. Tonnarelli, A. Papadimitropoulos, A. Scherberich, S. Schaeren, A. Schauerte, et al., Recapitulation of endochondral bone formation using human adult mesenchymal stem cells as a paradigm for developmental engineering 107 (16) (2010) 7251.

[162] J. van der Stok, M.K. Koolen, H. Jahr, N. Kops, J.H. Waarsing, H. Weinans, et al., Chondrogenically differentiated mesenchymal stromal cell pellets stimulate endochondral bone regeneration in critical-sized bone defects, Eur. Cells Mater. 27 (2014) 137–148, discussion 48.

[163] M. Sarem, O. Otto, S. Tanaka, V.P. Shastri, Cell number in mesenchymal stem cell aggregates dictates cell stiffness and chondrogenesis, Stem Cell Res. Ther. 10 (1) (2019) 10.

[164] A.M. McDermott, S. Herberg, D.E. Mason, J.M. Collins, H.B. Pearson, J. H. Dawahare, et al., Recapitulating bone development through engineered mesenchymal condensations and mechanical cues for tissue regeneration, Sci. Transl. Med. 11 (495) (2019), eaav7756.

[165] G. Nilsson Hall, L.F. Mendes, C. Gklava, L. Geris, F.P. Luyten, I. Papantoniou, Developmentally engineered callus organoid bioassemblies exhibit predictive in vivo long bone healing, Adv. Sci. (Weinheim, Ger.) 7 (2) (2019) 1902295.

[166] J. Groll, J.A. Burdick, D.W. Cho, B. Derby, M. Gelinsky, S.C. Heilshorn, et al., A definition of bioinks and their distinction from biomaterial inks, Biofabrication 11 (1) (2018), 013001.

[167] D.N. Heo, B. Ayan, M. Dey, D. Banerjee, H. Wee, G.S. Lewis, et al., Aspiration-assisted bioprinting of co-cultured osteogenic spheroids for bone tissue engineering, Biofabrication 13 (1) (2020), 015013.

[168] N.I. Moldovan, N. Hibino, K. Nakayama, Principles of the kenzan method for robotic cell spheroid-based three-dimensional bioprinting<sup/>, Tissue Eng. B Rev. 23 (3) (2017) 237–244.

[169] A. McCormack, C.B. Highley, N.R. Leslie, F.P.W. Melchels, 3D printing in suspension baths: keeping the promises of bioprinting afloat, Trends Biotechnol. 38 (6) (2020) 584–593.

[170] A.M. Compaan, K. Song, Y. Huang, Gellan fluid gel as a versatile support Bath material for fluid extrusion bioprinting, ACS Appl. Mater. Interfaces 11 (6) (2019) 5714–5726.

[171] O. Jeon, Y.B. Lee, H. Jeong, S.J. Lee, D. Wells, E. Alsberg, Individual cell-only bioink and photocurable supporting medium for 3D printing and generation of engineered tissues with complex geometries, Mater Horiz. 6 (8) (2019) 1625–1631.

[172] M. Hospodiuk, K.K. Moncal, M. Dey, I.T. Ozbolat, Extrusion-based biofabrication in tissue engineering and regenerative medicine, in: A. Ovsianikov, J. Yoo, V. Mironov (Eds.), 3D Printing and Biofabrication, Springer International Publishing, Cham, 2016, pp. 1–27.

[173] B. Ayan, D.N. Heo, Z. Zhang, M. Dey, A. Povilianskas, C. Drapaca, et al., Aspiration-assisted bioprinting for precise positioning of biologics, Sci. Adv. 6 (2020), eaaw5111-eaaw5111, https://doi.org/10.1126/sciadv.aaw5111.

[174] B. Ayan, Y. Wu, V. Karuppagounder, F. Kamal, I.T. Ozbolat, Aspiration-assisted bioprinting of the osteochondral interface, Sci. Rep. 10 (1) (2020) 13148.

[175] N.V. Mekhileri, K.S. Lim, G.C.J. Brown, I. Mutreja, B.S. Schon, G.J. Hooper, et al., Automated 3D bioassembly of micro-tissues for biofabrication of hybrid tissue engineered constructs, Biofabrication 10 (2) (2018), 024103.

[176] D. Murata, R. Fujimoto, K. Nakayama, Osteochondral regeneration using adipose tissue-derived mesenchymal stem cells, Int. J. Mol. Sci. 21 (10) (2020).

[177] A. Yamasaki, Y. Kunitomi, D. Murata, T. Sunaga, T. Kuramoto, T. Sogawa, et al., Osteochondral regeneration using constructs of mesenchymal stem cells made by bio three-dimensional printing in mini-pigs, J. Orthop. Res. 37 (6) (2019) 1398–1408.

[178] S.P. Grogan, E.W. Dorthé, N.E. Glembotski, F. Gaul, D.D. D'Lima, Cartilage tissue engineering combining microspheroid building blocks and microneedle arrays, Connect. Tissue Res. 61 (2) (2020) 229–243.

[179] Á.E. Mercado-Pagán, A.M. Stahl, Y. Shanjani, Y. Yang, Vascularization in bone tissue engineering constructs, Ann. Biomed. Eng. 43 (3) (2015) 718–729.

[180] C. Twohig, M. Helsinga, A. Mansoorifar, A. Athirasala, A. Tahayeri, C.M. França, et al., A dual-ink 3D printing strategy to engineer pre-vascularized bone scaffolds in-vitro, Mater. Sci. Eng. C 123 (2021), 111976.

[181] D.N. Heo, M. Hospodiuk, I.T. Ozbolat, Synergistic interplay between human MSCs and HUVECs in 3D spheroids laden in collagen/fibrin hydrogels for bone tissue engineering, Acta Biomater. 95 (2019) 348–356.

[182] B. Akar, B. Jiang, S.I. Somo, A.A. Appel, J.C. Larson, K.M. Tichauer, et al., Biomaterials with persistent growth factor gradients in vivo accelerate vascularized tissue formation, Biomaterials 72 (2015) 61–73.

[183] Z. Wang, Z. Wang, W.W. Lu, W. Zhen, D. Yang, S. Peng, Novel biomaterial strategies for controlled growth factor delivery for biomedical applications, NPG Asia Materials 9 (10) (2017), e435-e.

[184] M.A. Kuss, S. Wu, Y. Wang, J.B. Untrauer, W. Li, J.Y. Lim, et al., Prevascularization of 3D printed bone scaffolds by bioactive hydrogels and cell co-culture, J. Biomed. Mater. Res. B Appl. Biomater. 106 (5) (2018) 1788–1798.

[185] Y. Deng, C. Jiang, C. Li, T. Li, M. Peng, J. Wang, et al., 3D printed scaffolds of calcium silicate-doped β-TCP synergize with co-cultured endothelial and stromal cells to promote vascularization and bone formation, Sci. Rep. 7 (1) (2017) 5588.

[186] B.M. Roux, B. Akar, W. Zhou, K. Stojkova, B. Barrera, J. Brankov, et al., Preformed vascular networks survive and enhance vascularization in critical sized cranial defects, Tissue Eng. A 24 (21–22) (2018) 1603–1615.
[187] M.A. Skylar-Scott, S.G.M. Uzel, L.L. Nam, J.H. Ahrens, R.L. Truby, S. Damaraju, et al., Biomanufacturing of organ-specific tissues with high cellular density and embedded vascular channels, Sci. Adv. 5 (9) (2019), eaaw2459.
[188] J.A. Brassard, M. Nikolaev, T. Hübscher, M. Hofer, M.P. Lutolf, Recapitulating macro-scale tissue self-organization through organoid bioprinting, Nat. Mater. 20 (1) (2021) 22–29.
[189] X. Liu, W. Chen, C. Zhang, W. Thein-Han, K. Hu, M.A. Reynolds, et al., Co-seeding human endothelial cells with human-induced pluripotent stem cell-derived mesenchymal stem cells on calcium phosphate scaffold enhances osteogenesis and vascularization in rats, Tissue Eng. A 23 (11–12) (2017) 546–555.
[190] S. Li, K. Wang, Q. Hu, C. Zhang, B. Wang, Direct-write and sacrifice-based techniques for vasculatures, Mater. Sci. Eng. C 104 (2019), 109936.
[191] A.A. Gorkun, D.P. Revokatova, I.M. Zurina, D.A. Nikishin, P.Y. Bikmulina, P. S. Timashev, et al., The duo of osteogenic and angiogenic differentiation in ADSC-derived spheroids, Front. Cell Dev. Biol. 9 (2021), 572727.
[192] S. Inglis, J.M. Kanczler, R.O.C. Oreffo, 3D human bone marrow stromal and endothelial cell spheres promote bone healing in an osteogenic niche 33 (3) (2019) 3279–3290.
[193] H. Chaddad, S. Kuchler-Bopp, G. Fuhrmann, H. Gegout, G. Ubeaud-Sequier, P. Schwinté, et al., Combining 2D angiogenesis and 3D osteosarcoma microtissues to improve vascularization, Exp. Cell Res. 360 (2) (2017) 138–145.
[194] Y. Zhang, P. Kumar, S. Lv, D. Xiong, H. Zhao, Z. Cai, et al., Recent advances in 3D bioprinting of vascularized tissues, Mater. Des. 199 (2021), 109398.